UTILIZING MICROSTIMULATION AND LOCAL FIELD POTENTIALS IN THE PRIMARY SOMATOSENSORY AND MOTOR CORTEX

by

Jason Godlove

B.S. Biology, University of Maryland, Baltimore County 2004

Submitted to the Graduate Faculty of

Swanson School of Engineering in partial fulfillment

of the requirements for the degree of

Doctor of Philosophy

University of Pittsburgh

2013

UNIVERSITY OF PITTSBURGH

SWANSON SCHOOL OF ENGINEERING

This dissertation was presented

by

Jason Godlove

It was defended on

September 16th, 2013

and approved by

Douglas Weber, Ph.D., Associate Professor, Dept. of Bioengineering

Neeraj Gandhi, Ph.D., Associate Professor, Dept. of Bioengineering

Satish Iyengar, Ph.D., Professor and Chair, Dept. of Statistics

Dissertation Director: Aaron Batista, Ph.D., Assistant Professor, Dept. of Bioengineering

UTILIZING MICROSTIMULATION AND LOCAL FIELD POTENTIALS IN THE PRIMARY SOMATOSENSORY AND MOTOR CORTEX

Jason Godlove, Ph.D.

University of Pittsburgh, 2013

Brain-computer interfaces (BCIs) have advanced considerably from simple target detection by recording from a single neuron, to accomplishments like controlling a computer cursor accurately with neural activity from hundreds of neurons or providing instruction directly to the brain via microstimulation. However as BCIs continue to evolve, so do the challenges they face. Most BCIs rely on visual feedback, requiring sustained visual attention to use the device. As the role of BCIs expands beyond cursors moving on a computer screen to robotic hands picking up objects, there is increased need for an effective way to provide quick feedback independent of vision. Another challenge is utilizing all the signals available to produce the best decoding of movement possible. Local field potentials (LFPs) can be recorded at the same time as multi-unit activity (MUA) from multielectrode arrays but little is known in the area of what kind of information it possess, especially in relation to MUA. To tackle these issues, we preformed the following experiments.

First, we examined the effectiveness of alternative forms of feedback applicable to BCIs, tactile stimuli delivered on the skin surface and microstimulation applied directly to the brain via the somatosensory cortex. To gauge effectiveness, we used a paradigm that captured a fundamental element of feedback: the ability to react to a stimulus while already in action. By measuring the

response time to that stimulus, we were able to compare how well each modality could perform as a feedback stimulus.

Second, we use regression and mutual information analyses to study how MUA, low-frequency LFP (15-40Hz, LFP_L), and high-frequency LFP (100-300Hz, LFP_H) encoded reaching movements. The representation of kinematic parameters for direction, speed, velocity, and position were quantified and compared across these signals to be better applied in decoding models.

Lastly, the results from these experiments could not have been accurately obtained without keeping careful account of the mechanical lags involved. Each of the stimuli affecting behavior had onset lags, which in some cases, varied greatly from trial to trial and could easily distorted timing effects if not accounted for. Special adaptations were constructed to precisely pinpoint display, system, and device onset lags.

TABLE OF CONTENTS

LIST OF TABLES

LIST OF FIGURES

PREFACE

The work in Chapter 2 is in the final stages of preparation. Chapter 3 has already been published. Chapter 4 is to serve as a reference guide for future members of the Batista lab. Accompanying this dissertation is a flash drive containing material discussed in this document as well as other projects I was involved with, of which a complete list can be found in Appendix A.

Chapter 2: Godlove JM, O'Brien E, Batista AP. Comparing temporal aspects of visual, tactile, and microstimulation feedback for motor control. *In preparation.*

Chapter 3: Perel S, Sadtler PT, Godlove JM, Ryu SI, Wang W, Batista AP, Chase SM. Direction and Speed Tuning of Motor-Cortex Multi-Unit Activity and Local Field Potentials During Reaching Movements. *Proceedings of the 35th Annual International IEEE EMBS Conference*. July 3-7, 2013, Osaka, Japan. 1247.

Acknowledgements

First and foremost, I wish to thank my advisor, Aaron Batista. I've had an amazing experience working in his lab since the beginning, building it from the ground up. I've learned so much from him about science and about life. He is an excellent advisor and a good friend. Thank you to my thesis committee, Doug Weber, Raj Gandhi, and Satish Iyengar. Their insightful and unique feedback helped me view my project from different angles and become a well-rounded scientist. I couldn't have asked for a better team to both challenge and guide me.

I wish to thank Steve Chase and Sagi Perel for a very rewarding collaboration; I learned so much from their excellent teaching skills. A special thanks to Melissa James, Erin O'Brien, and

Brian Hu, who assisted me in my projects, without them, I would still be here for another 6 years. To Kennedy, Lincoln, and McKinley for all that they've done. I couldn't have gotten here without their help and hard work. They taught me the value of patience and how to adapt quickly to succeed. I will always admire Kennedy's keen mind, Lincoln's solid work ethic and I thank McKinley for being an excellent partner in research; I couldn't have done this work without him.

To Lisa Bopp, Darlene Thiel, and the other SNI members and support staff for always being there to answer my questions when I popped by. A special thanks to the CNBC program. Not only did they provide me with numerous grants and travel funds, but also they formed a close-knit community of neuroscientists that fostered fruitful collaborations and friendships that made coming to Pittsburgh an inspiring scientific experience.

And finally, I wish to thank my family for all the support they've given me over the years. I wouldn't be here if it wasn't for them always in my corner.

1.0 GENERAL INTRODUCTION

For almost two centuries, electrical microstimulation has been a useful tool in exploring the organization and function of the nervous system. Perturbing neural activity has been invaluable in probing system components for their contribution and function, particularly in the motor systems. It has been used to explore specific populations of neurons and how they contribute to cognitive and sensory processing within a system. Microstimulation has been used in numerous studies to activate motor pathways and cause a behavioral response as well in stimulating sensory pathways to be behaviorally detected. These studies give a glimpse into how the brain structures interact with one another and process information.

1.1 ELECTRICAL MICROSTIMULATION

In 1870, Fritsch & Hitzig discovered that when electrical stimulation was applied to the surface of a dog's cortex, it evoked discrete movements that were repeatable with sequent stimulations. When stimulation, in the form of brief pulses of direct current, was applied to different areas of the cortex, it would evoke different muscle groups depending on the area. This was the first evidence that specific functions could be localized in the brain (Fritsch & Hitzig, 1870).

Since then, microstimulation has evolved from direct current applied via a battery, to a more precise tool that can produce reliable activation with minimal neural tissue damage (Fritsch

& Hitzig, 1870; Tehovnik, 1996). For instance, most experiments use biphasic pulses composed of equal duration anodal and cathodal phases so that no net charge is left to do electrolytic damage to the stimulated tissue (Tehovnik, 1996). Experimenters have altered the pulse duration, polarity, inter-pulse interval, current amplitude, and temporal sequencing of the pulse in order to adjust the efficacy of the microstimulation. Stimulation frequencies typically range from 20-400 Hz with current amplitudes ranging from 5-500μA.

The current flowing from the electrode tip and changing the membrane potential of the surrounding neurons causes the direct effect of microstimulation. The level of change in the membrane potential drops off at an exponential rate the further the neuronal element is from the tip (Rattay, 1999). This direct effect can depolarize cells enough to make them spike or affect the probability a neuron will spike in the future through inhibition or sub-threshold excitation. These spikes can indirectly trigger a vastly larger amount of spiking events than what was initially triggered by the microstimulation event (London, et al., 2010). Using one electrode to stimulate and another to record, it was reported that a 200μs cathodal pulse of 10μA directly activated most neurons within 90μm of the stimulating electrode's tip (Stoney, et al., 1968). Increased amplitudes from 2 to 150μA would activate within 50-500μm from the tip, corresponding to roughly 60-62,000 neurons in monkey V1 (Tehovnik & Slocum, 2007).

1.2 EVOKING SENSATIONS

In early experiments with conscious human patients, it was found that when points on the occipital cortex were stimulated, patients reported seeing localized spots of lights called phosphenes at

particular locations that varied depending on where the stimulation was applied (Brindley GS & Lewin WS, 1968). In the primary visual cortex (V1), the sensation of localized blindness has been produced via microstimulation (Penfield, 1958). While monkeys are unable to describe visual percepts created by microstimulation in V1, its effect on the visual system was reflected by the behavior exhibited such as eye-movements to the receptive field of the stimulated area, interfere with visual tasks, or by animals trained to report the presence of microstimulation (Bartlett & Doty, 1980)**.** The success and reliability of these tasks was always proportional to the amplitude of the stimulation current, with different brain areas requiring different amplitude thresholds to induce the same level of performance (Murphey & Maunsell, 2007; Murphey & Maunsell, 2008).

Microstimulation has also been used to elucidate the role of the primary somatosensory cortex in tactile discrimination. Romo *et al.* (Romo, et al., 1998) conducted discrimination experiments where monkeys compared the frequency of tactile stimuli to the fingertips during two intervals. The monkeys would then report which of the two intervals contained the higher frequency of stimulation. During the progress of the experiment, one of the tactile stimuli was replaced with microstimulation of the somatosensory cortex, requiring a comparison between the frequency of a physical and an electrical stimulus. Surprisingly, the animals were able to do the task to the level of performance of when both stimuli were physical. Further studies eventually had the monkeys discriminating two intervals of microstimulation with each other with notable success (Romo, et al., 2000).

1.3 EVOKING MOVEMENTS

1.3.1 Evoked Eye Movements

Stimulation of the frontal eye field (FEF) and of the superior colliculus (SC) produces precise saccadic eye movements in the direction of their respective receptive field (Robinson, 1972; Robinson & Fuchs, 1969). The amplitude and direction of the saccades vary systematically according to the stimulating electrodes position within the FEF (figure 1). In animals without head restraint, microstimulation of FEF produces gaze shifts that combine eye and head movements in a manner similar to naturally produced gaze shifts (Knight & Fuchs, 2007).

While the position of the electrode affects the direction and ultimately the end point of the evoked saccade, varying the stimulus frequency, amplitude, and pulse train duration seem to only affect the probability of evoking a saccade (Robinson, 1972; Schiller & Stryker, 1972; Bruce, et al., 1985). The pattern of current-pulse timing can have an interesting effect on saccade probability from microstimulation of the FEF. Kimmel & Moore stimulated the FEF with five different patterns of pulse timings, each lasting 35ms with eight pulses, but different pulse distributions across the stimulus duration. The interpulse-intervals (IPIs) could be uniform (fixed), increasing (decelerating), decreasing (accelerating), or random (figure 2a). They found the different patterns displayed disparate efficacy in evoking saccades. When the eight pulses were arranged in an accelerating pattern, saccades were evoked more readily than if the pulses were arranged in a decelerating pattern (figure 2b). This shows that the oculomotor system is highly sensitive to the relative timing of pulses even within a small time frame (Kimmel & Moore, 2007).

In addition to studying saccadic eye movements, microstimulation has been used to study oculomotor vergence and pursuit (figure 1a). Short-latency vergence movements are produced from microstimulation of a region just anterior to the FEF (Gamlin & Yoon, 2000). Stimulation of a sub-region of the FEF in the fundus of the arcuate sulcus produces smooth eye movements and modifies the gains of movements used for pursuit (Gottlieb, et al., 1993; Tanaka & Lisberger, 2002).

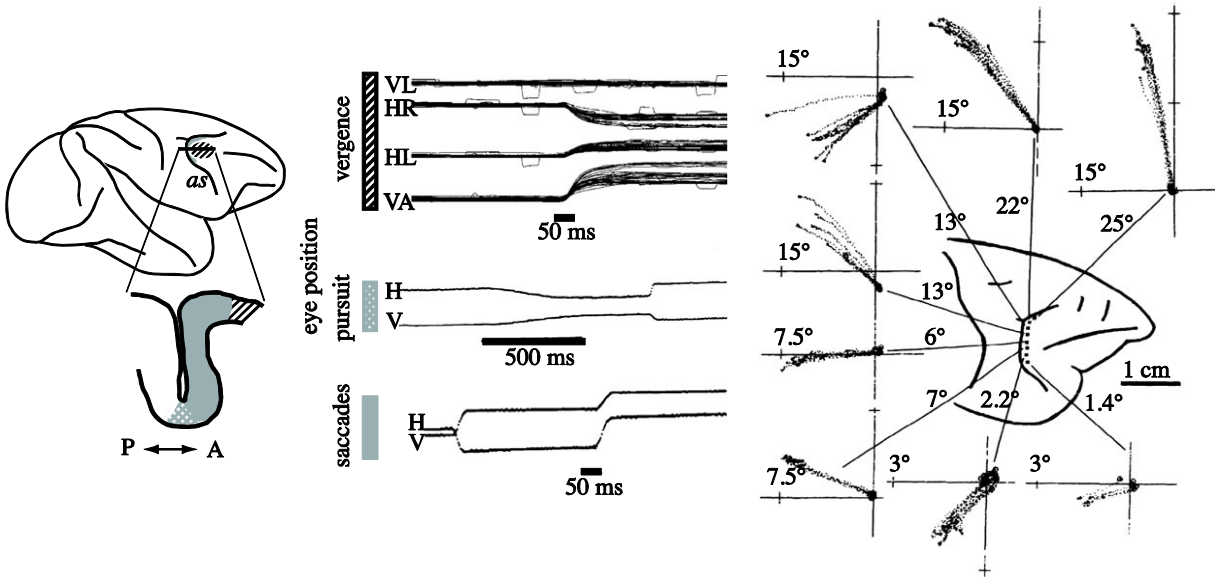

Figure 1. Evoking eye movements with microstimulation.

Microstimulation of different regions inside and surrounding the arcuate sulcus (as) produces vergence (striped), smooth pursuit (plaid) and saccadic (solid) eye movements. Map of saccade amplitudes and directions evoked by microstimulation of the frontal eye field sites shown. Abbreviations: P, posterior; A, anterior; VL, vertical left; HR, horizontal right; HL, horizontal left; VA, vergence angle; H, horizontal; V, vertical. Adapted from (Clark, et al., 2011; Bruce, et al., 1985; Gamlin & Yoon, 2000; Gottlieb, et al., 1993)

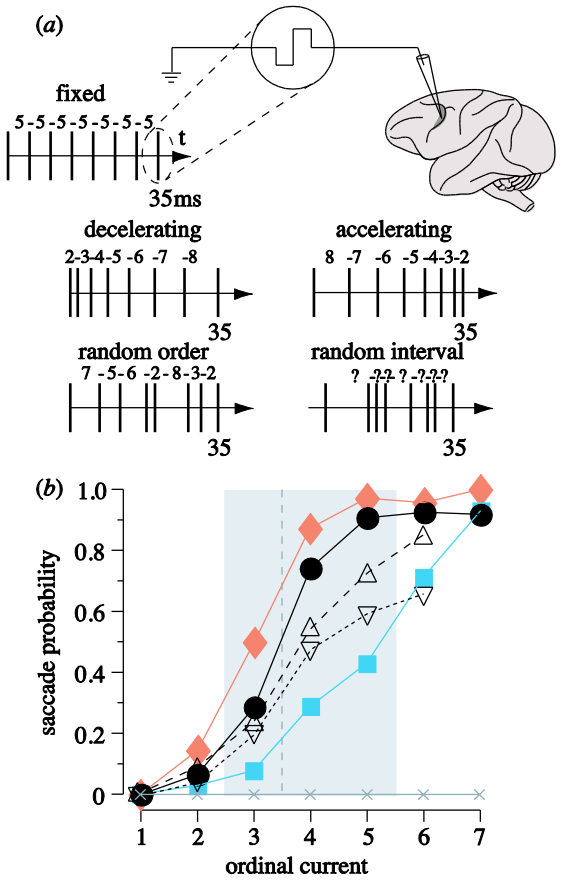

Figure 2. Varying the temporal pattern of microstimulation.

(a) FEF was stimulated with pulse trains of 35 ms duration and a total of eight bimodal pulses; individual IPIs, in milliseconds, are displayed above each train (question marks denote random IPIs). IPIs were uniform (fixed, black circles), increasing (decelerating, blue squares), decreasing (accelerating, red diamonds), random order (RO, triangles), or random intervals (RIs, inverted triangles). (b) Average probability of evoking a saccade as a function of ordinal current (relative to site threshold, depicted by grey dotted line) at 14 FEF sites. All pairwise comparisons between patterns over the middle range of currents (shaded in grey) yielded significant differences except the two random patterns. Grey crosses, no stimulation. Adapted from (Clark, et al., 2011; Kimmel & Moore, 2007).

1.3.2 Evoked Hand Movements

When stimulating in the somatic motor cortex, distinct movements or muscle activations are seen for stimulations sites only a few hundred microns apart (Asanuma & Rosén, 1972; Donoghue & Wise, 1982; Neafsey, et al., 1986). This, along with its clearly seen behavioral response, attributes to how this was the first area to have its functional organization mapped with electrical stimulation (Fritsch & Hitzig, 1870; Penfield, 1958; Ferrier, 1876). Many studies observed muscle twitches from short stimulation durations (typically <50ms) (Asanuma & Sakata, 1967; Strick & Preston, 1978). Graziano *et al.*(2002) investigated the effects of longer (500ms) stimulus durations in the arm area of motor and premotor cortex (PM); a timescale similar to full arm movements. The longer trains of microstimulation evoked full coordinated body movements from multiple joints to reach to a final fixed posture. For example, 500ms stimulation at one site would cause the monkey to bring its hand toward the mouth with a closed, grip-like hand posture and open its mouth, regardless of initial position (figure 3). Although these movements occurred over the span of a several hundred millisecond stimulus train, EMG recordings of muscle activation have measured response to the train as little as 7ms after stimulus onset (Graziano, et al., 2004). Additionally, velocity profiles for the movement were similar to those of spontaneous natural movements.

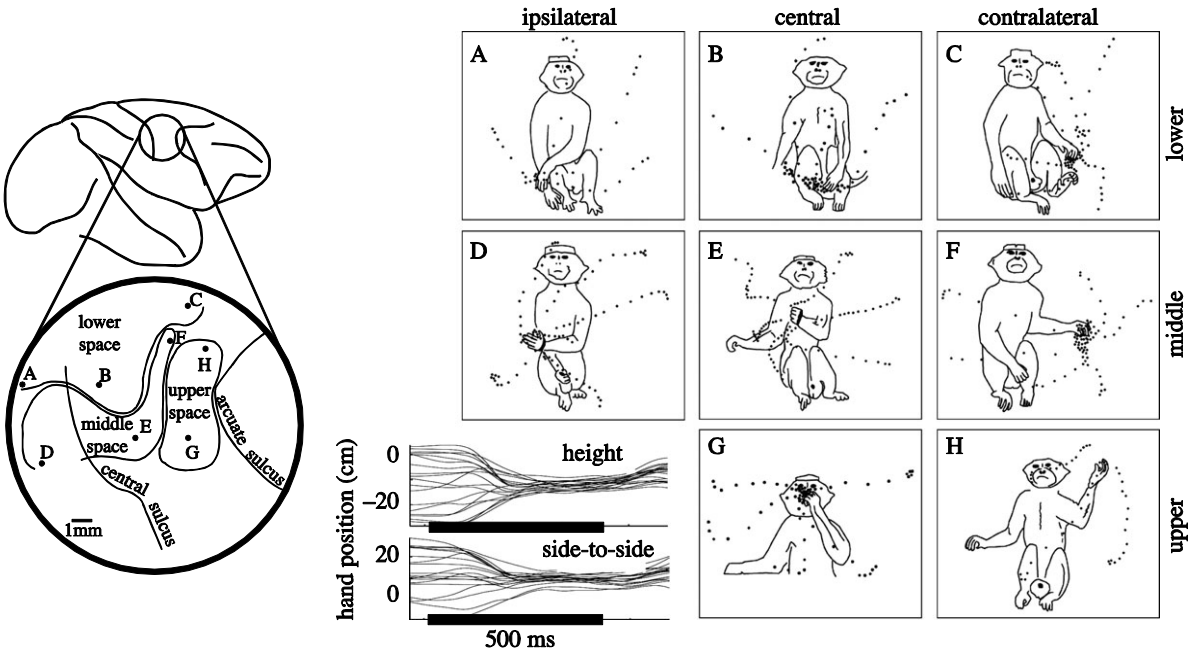

Figure 3. Evoking arm and hand movements with microstimulation.

Microstimulation of motor and premotor for 500 ms evoked complex, coordinated movements terminating in a fixed final posture regardless of the initial position. Left: traces show hand position during microstimulation. (A–H): map of arm movements evoked by microstimulation of the motor and premotor sites shown. Dotted lines indicate path of hand movement, ending in the position shown. Adapted from (Clark, et al., 2011; Graziano, et al., 2002; Graziano, et al., 2004)

1.4 DETECTING CORTICAL MICROSTIMULATION

The majority of studies describing behavioral report of microstimulation have occurred in the primary sensory or motor cortex. When the primary sensory cortex is stimulated, human subjects have reported the appearance of phosphenes, or other basic sensations. Animals can also be trained to report when the primary sensory cortex is stimulated (Bartlett & Doty, 1980; Tehovnik, et al., 2006; Murphey & Maunsell, 2007). In most experiments, there was little attempt to understand

what the animals experienced during microstimulation with the exception of Romo and colleagues (2000). Their work forced the subjects to directly compare tactile stimuli with the percepts produced by microstimulation of area 3b in primary somatosensory cortex with remarkable success. Following experiments have shown that monkeys can also discriminate frequencies of microstimulation in areas 1 and 3a (O'Doherty, et al., 2011; London, et al., 2008).

Several studies have shown that animals can detect microstimulation just about anywhere in the cortex, not just the primary sensory areas (Doty, 1969). However, it should be noted that extensive training was required before animals could reliably detect microstimulation in non-primary areas. Fitzsimmons *et. al.* (2007) reported similar difficulties when stimulating in area 1 of the primary somatosensory cortex. Because stronger stimulation current directly excites more neurons, measuring the amount of current needed for a stimulus to be detected gives a good indication of how many cortical neurons must be activated before the subject can detect the microstimulation. Murphey and Maunsell (2007) trained monkeys to detect microstimulation applied to numerous cortical areas. After extensive training, they found little difference in detection thresholds across the visual cortex (~6μA) about V1 or across FEF (~14μA) (Murphey & Maunsell, 2008).

With practice, lower thresholds can be obtained for detecting microstimulation. This comes as little surprise because trains of electrical stimuli are commonly used to evoke long-term potentiation or depression of neuronal connections in culture or slice experiments (Heusler, et al., 2000). In vivo, microstimulation has been shown to alter response properties of cortical neurons, making them more or less receptive to specific stimuli (Frégnac, et al., 1988), or by changing the

orientation map in V1 (Dinse, et al., 1997; Godde, et al., 2002), or somatotopic map in area 3b (Jenkins, et al., 1990). In behavioral experiments, evidence of plasticity has been shown with reduced thresholds for stimulus detection in V1 after extensive practice. Interestingly, these improved levels of stimulus detection strongly correspond to the immediate area of stimulation, with surrounding areas left indifferent when stimulated unless previously trained for microstimulation there (Doty, et al., 1956; Doty, 1965; Bartlett & Doty, 1980). Ni *et. al.* (2010) showed similar results with V1 microstimulation. Animals could always easily detect strong V1 stimulation, but when the stimulation was relatively week and near detection threshold, improvement could be seen over time. Figure 4a shows the monkey could not initially detect stimulation trains of 50μA but over the course of about 10 days of training, detection thresholds dropped to 6μA. This improvement was primarily seen when stimulating in the same 3mm x 3mm area over multiple days with animals that already had extensive training with the task. Figure 4b demonstrates the detection thresholds when stimulating 10mm away from the trained stimulated area. While some generalization can be detected, thresholds were still high and multiple training sessions were required to reduce the threshold (Ni & Maunsell, 2010). This threshold training effect was also seen when stimulated areas of area 3a of the somatosensory cortex in multiple sites only a few mm away (London, et al., 2008). These learning effects remained present even in the absence of stimulation in that area for over a year (gap in the data in figure 4b**).**

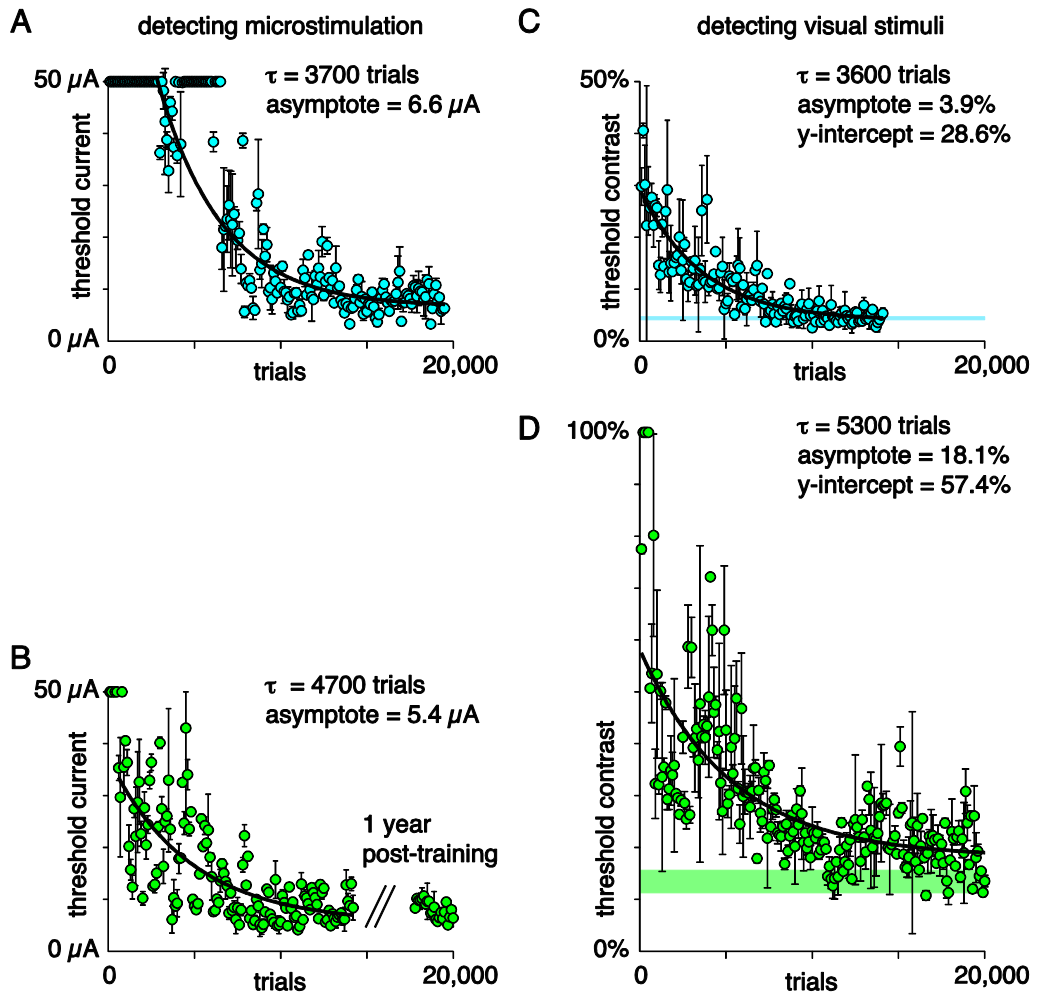

Figure 4. Effects of training to detect microstimulation of V1.

(A) Threshold current needed for behavioral detection of stimulation of a small 3mm x 3mm region in V1 as a function of time over the course of many days. (B) After training the site in A, electrical stimulation at a distant V1 site required retraining to achieve low thresholds. Thresholds were stable for over a year without further training at this site. (C) After training to detect electrical stimulation at the site in A, visual stimuli detection at the corresponding retinal location was impaired with thresholds far above the normal range (marked by the thin horizontal band), but gradually returned to normal after practice. (D) Retraining with visual stimuli at site A did not improve visual detection at site B, but improved after practice with visual stimuli in that retinal location. The horizontal band marks the range of normal visual thresholds for this site. Adapted from (Histed, et al., 2013; Ni & Maunsell, 2010).

The fact that training to detect microstimulation to lower detection thresholds is similar to training to detect a novel perceptual stimulus suggests that the cortex treats microstimulation like a new natural stimulus. This improvement over tens of thousands of trials is unlikely to be caused from the animal simply discovering that the stimulus is associated with the reward. It is more likely that this gradual improvement is from the subjects slowly acquiring the ability to perceive the stimulus, like eyes adjusting to the dark. This could be brought about in two ways. First, detection may require a set number of neurons to be activated through stimulation, and with training, the intrinsic neuronal properties of neurons in that area are altered to be more excitable to repeated stimulus. Alternately, the number of neurons activated by microstimulation does not change directly, however the synaptic connections to those neurons are altered to make them more sensitive to the spatiotemporal pattern of activation from repeated microstimulation (Histed, et al., 2013). This synaptic modification rather than neuronal excitability is supported by studies in rat behavioral thresholds for detecting functional connectivity between neurons in regions of stimulation (Rebesco & Miller, 2011). Additionally, improvement in microstimulation detection in V1 has been coupled with a profound, yet selective impairment of visual detection of natural stimuli in the receptive field of the stimulated area. Figure 4c & d show the thresholds for detecting visual stimuli after microstimulation training is ~5 times normal levels. These increases in threshold were localized to the stimulated area, with surrounding areas threshold left unaffected. Luckily, these increased thresholds for detection could be returned to normal levels with repeated training with actual visual stimuli (Ni & Maunsell, 2010). The fact that the effect persisted until revered with non-invasive measures shows that the threshold increase was not due to tissue damage. This reciprocal relationship between visual and V1 microstimulation detection suggests that learning does not involve a simple increase in excitability of V1 which would raise sensitivity

to both stimuli, but a rewiring of limited cortical circuitry to favor microstimulation over visual stimuli, until trained otherwise.

The idea that the brain is predisposed to process particular spatiotemporal patterns of activity suggests an interesting dilemma for utilizing microstimulation of the primary sensory and motor cortex in brain computer interfaces. Unless used in an area where the electrical stimulation applied is adequately similar to the natural activity patterns of the stimulated area, it may create a decrease in actual sensory perception in order to increase perception for microstimulation. This primarily affects microstimulation's prospects as a rehabilitation tool if it cannot be pair with a natural movement or natural stimulus. On the other hand, it is reassuring that the brain can readily adapt to this novel and foreign sensory perception, incorporating it into its neural circuitry and improving detection over time.

1.5 EXPERIMENTAL AIMS

A primary goal of this dissertation is to evaluate various aspects of current brain-computer-interfaces, how they respond under closer scrutiny, and to understand the mechanisms behind their performance. We have three specific Aims:

Aim 1. Measure the response time to microstimulation of the primary somatosensory cortex

To effectively incorporate microstimulation as a feedback modality, we must first understand its strengths, shortcomings, and how well it compares alternative feedback modalities. In Chapter 2, we sought to demonstrate that microstimulation could be utilized quickly enough to affect a

movement in progress. The goal of Chapter 2 was to quantify how quickly a monkey could respond to a microstimulation cue mid-motion compared to visual and tactile stimuli in order to gauge microstimulation's effectiveness as a feedback modality.

Aim 2. Quantify the kinematic information contained in Local Field Potential and Multi-Unit Activity of the motor cortex

To develop better decoding algorithms for BCIs, we must first understand how to model the information contained in the recorded signals. In Chapter 3, we used regression and mutual information analyses to study how Multi-Unit-Activity (MUA) and Local Field Potentials (LFPs) encode various kinematic parameters during reaching movements. We then applied position, direction, speed, and velocity models (and combinations thereof) to MUA and LFP activity to better understand the information contained in each signal modality.

Aim 3. To tightly regulate and correct stimulus onset with the Real-Time system timing

Visual, tactile, and microstimulation stimuli each require a variable amount of time between when a signal is sent to turn on a stimulus and when that stimulus actually turns on. We designed devices to regulate these system lags so that timing characteristics of neural and behavioral responses could be assessed with minimal error. Chapter 4 explains how to construct and use the custom equipment for the behavioral rig and analyze the system signals to quantify lag associated with the visual, tactile, microstimulation, and Phasespace systems.

2.0 COMPARING TEMPORAL ASPECTS OF VISUAL, TACTILE, AND MICROSTIMULATION FEEDBACK FOR MOTOR CONTROL

2.1 ABSTRACT

Current brain-computer interfaces (BCIs) rely on visual feedback, requiring sustained visual attention to use the device. As BCIs improve, it increases the need for an effective way to provide quick feedback independent of vision. Tactile stimuli, either delivered on the skin surface, or directly to the brain via microstimulation in somatosensory cortex, could serve that purpose. We examined the effectiveness of vibrotactile stimuli and microstimulation by using a fundamental element of feedback: the ability to react to a stimulus while already in action. In human and monkey subjects, we found response to tactile cues was faster than visual cues. However, monkey response to microstimulation was the slowest of the three modalities. The temporal aspects of feedback are an important design constraint that should be included when designing alternative forms of feedback for brain-computer interfaces.

2.2 INTRODUCTION

Cortically controlled brain-computer interfaces (BCIs) were first demonstrated over ten years ago in humans and monkeys (Nicolelis, et al., 2003; Kennedy, et al., 2004; Suminski, et al., 2011). BCI control has been demonstrated in sophisticated behaviors such as cursor control (Jarosiewicz, et al., 2013; Musallam, et al., 2004; Li, et al., 2011; Gilja, et al., 2012; Kim, et al., 2008; Mulliken,

et al., 2008), self-feeding using a robotic arm (Hochberg, et al., 2012; Carmena, et al., 2003; Hochberg, et al., 2006; Velliste, et al., 2008), and the voluntary control of paralyzed muscles (Moritz, et al., 2008; Pohlmeyer, et al., 2009; Ethier, et al., 2012). While much has been accomplished, there is still room for improvement as we strive to achieve performance comparable to natural movement. One obstacle to more natural performance is that most current BCI paradigms rely on vision as the sole source of feedback.

Similarly, human subjects who have lost proprioception and touch and who must rely solely on vision can still move, however it requires great concentration and produces movements that are slow and inaccurate (Ghez, et al., 1995; Sainburg, et al., 1995; Cole, 1995). In able-bodied individuals, certain actions, like grip force when picking up an object, are controlled largely under non-visual feedback modalities. Next-generation BCIs will attain a higher degree of control once they incorporate other relevant sensory modalities such as tactile and proprioceptive feedback (Weber, et al., 2012; Suminski, et al., 2011).

Numerous studies have shown that tactile stimuli can improve performance in a wide range of tasks (Prewett, et al., 2006; Prewett, et al., 2012), including driving (Scott & Gray, 2008), stimulus detection reaction time paradigms (Forster, et al., 2002; Diederich & Colonius, 2004), and target indication in BCI paradigms (Chatterjee, et al., 2007). We extended the use of tactile stimuli to a new context: as a feedback modality to alter a reach in progress. We quantified the effectiveness of tactile stimuli as a feedback modality by comparing it to vision.

Microstimulation in primary somatosensory cortex (S1) activates many of the same cortical pathways as tactile stimuli and, while cortical microstimulation is only beginning to be applied in a BCI context (O'Doherty, et al., 2011), microstimulation in sensory cortex has a long history as a method of providing sensory information (Weber, et al., 2012; London, et al., 2008; O'Doherty, et al., 2009; O'Doherty, et al., 2011; Fitzsimmons, et al., 2007). Ample evidence suggests microstimulation evokes sensory effects that mimic the functional contribution of the stimulated area (Salzman CD & Newsome WT, 1994; Romo, et al., 1998; Romo, et al., 2000; Romo, et al., 2002; Tehovnik, 1996; Graziano, et al., 2002; Cohen & Newsome, 2004; DeAngelis & Newsome, 2004; Tehovnik, et al., 2006; Liu & Newsome, 2000). Microstimulation in humans has been used to induce visual (Brindley GS & Lewin WS, 1968 ; Dobelle, et al., 1976), and tactile perceptions (Davis, et al., 1998; Kiss, et al., 2003; Ohara, et al., 2004). The effectiveness in microstimulation to provide sensory substitution leads us to expect that the reaction time to S1 microstimulation could be similar to that of tactile stimuli or even faster due to bypassing afferent pathways.

Previous studies utilizing microstimulation during hand control or BCI control have all applied it when the subject was at a state of rest, whether it be before movement onset (Fitzsimmons, et al., 2007; Romo, et al., 1998; Romo, et al., 2000), or when the subject lingered over a target area (O'Doherty, et al., 2011; O'Doherty, et al., 2009). The emphasis of those studies was placed on elucidating the discrimination thresholds between two different stimuli and testing the robustness of the information channel. Subjects were never required to utilize the stimulus during a movement to change the movement plan; the very essence of feedback. In order for microstimulation to be used successfully as an artificial sensory feedback channel, it must be able to be delivered and interpreted quickly enough for it to be utilized during ongoing movements.

Here we compare the temporal aspects of three different sensory modalities as sources of feedback about movement. We defined the elemental form of feedback as the ability of a subject to change an ongoing reach when confronted with new sensory information. To this end, we used a modified center-out reach task in which the subject's ongoing reach was occasionally interrupted by a stimulus cue that instructed an immediate change in reach goal. In both humans and monkeys, the response to tactile stimuli was faster than to visual stimuli. Surprisingly we found that the behavioral response to microstimulation in S1 was 25 percent slower than for visual stimuli. These results set a realistic basis of expectation for feedback modalities in behavioral and BCI applications.

2.3 MATERIALS AND METHODS

2.3.1 Basic Experimental Procedures

Human subjects were seated ~1m in front of a computer monitor so they could make unrestricted arm movements. Monkeys were seated in a primate chair; head-fixed with a modified halo system (Davis, et al., 2009) with the non-reaching arm loosely restrained. Monkeys sat in front of a mirror and performed the task in a virtual reality environment with the hand moving freely in the space behind the mirror. For humans and monkeys, hand position was represented by an onscreen cursor. Both humans and monkeys wore active motion capture markers (Phasespace, San Leandro, CA) on the index finger to record movements at 120Hz. Unrestricted hand movements occurred in a 1m x 1m empty workspace with the virtual workspace centered on the reaching hand's resting

position and reach targets adjusted to span a comfortable reaching range. Human reach distances from the center to the target were 25cm; monkeys 1 and 2 reached 12.5cm and 15cm respectively.

2.3.1.1 Human Subjects

Ten subjects (6 women, 4 men, ages 20-32 years) participated in the experiment. Participants gave informed consent before the start of the experiment and conformed to the guidelines of the University of Pittsburgh Institutional Review Board. Subjects trained until proficient (>70% success rate for redirect trials) over 1-2 short training sessions. Customized timing parameters were calculated for the subject to efficiently sample the entire reach span during the redirect task. The data used for analysis were collected during a final session of 1000 trials. To ensure that there were not ongoing learning effects that improved response times, two subjects participated in additional long sessions. Their response times improved between the training session and first long session then remained consistent in subsequent long sessions. Thus we used the first long session for all subjects.

2.3.1.2 Non-Human Primate Subjects

Two adult male Rhesus monkeys, 1 and 2 (Macaca mulatta, 8.4 and 10.4 kg) participated in this study. All animal procedures were reviewed and approved by the University of Pittsburgh's Institutional Animal Care and Use Committee, in accordance with US Department of Agriculture, International Association for the Assessment and Accreditation of Laboratory Animal Care, and National Institutes of Health guidelines.

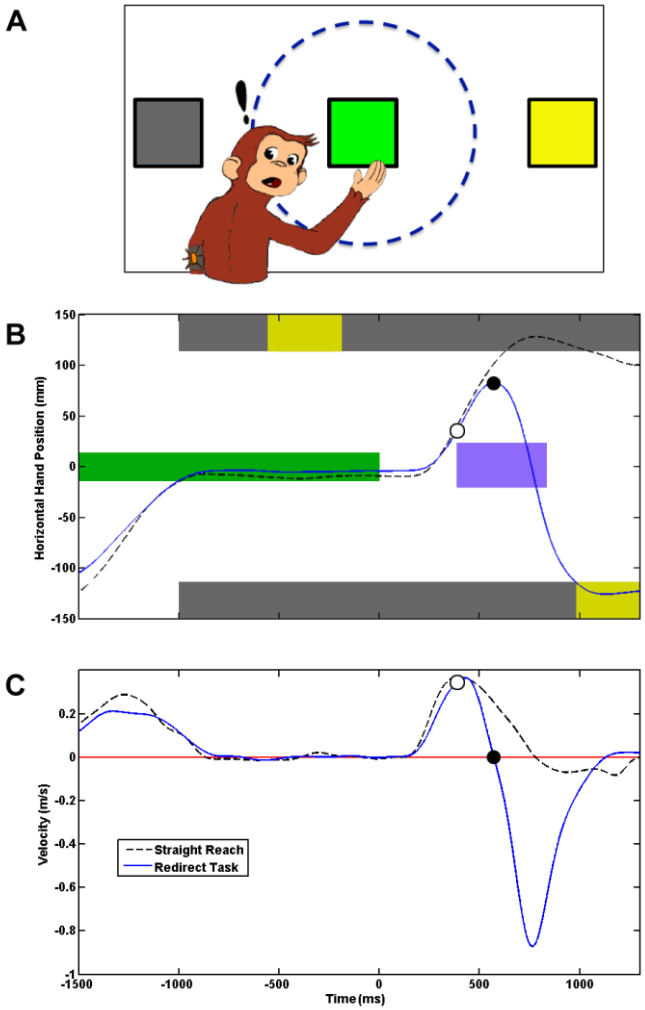

Figure 5. Experimental paradigm.

(a) Task configuration showing center start target (green), potential reach target (gray), and instructed reach target (yellow). The subject moved the hand to position a cursor on the target. Mid-reach redirect cues were given via vibrating motor, a blue circle, or microstimulation of S1. (b) Sample horizontal hand trajectory across time during a direct reach task (black dashed line) and a redirect task (solid blue line) with the go cue represented at time 0. Targets illustrated represent events from the redirect task, however target presentation during the direct reach task was identical up to onset of the redirect cue (blue). Position of the hand is marked at the redirect cue onset (°) and moment of reach inflection (•). (c) Horizontal hand velocity of the direct reach and redirect tasks. Response time to the redirect cue was measured as the time elapsed between redirect cue onset (°) and moment of reach inflection (•).

2.3.2 Behavioral Tasks

Our main behavioral task was a redirect task (described more fully below) in which a stimulus presented during an ongoing movement signaled a change in the goal location. The redirect task was randomly interleaved with a classic center-out reaching task, here called the direct reaching task. Our main quantification was the response time to the redirect stimulus, which indicates how rapidly a subject can respond to a stimulus as a source of feedback about an ongoing movement. We also employed a pressured reaction time task (described below) to assess how quickly the subject can respond to a particular stimulus.

2.3.2.1 Direct Reaching Task

Seventy percent of the trials were of a control task, performing a prompt reach to one of 2 possible opposing targets (figure 5a). Each trial began when the subject moved their hand to position a computer cursor into a central target (green square). Two peripheral grey squares then appeared indicating potential reach targets (figure 5b). One of the targets briefly flashed yellow to indicate the intended reach target. Disappearance of the start target signaled the subject to begin reaching. Movement began within a window of 80-400ms after the go cue to penalize false starts or lingering on the start target. The hand reached promptly and directly to the intended target within 800ms, or else the trial failed. Human subjects were instructed to reach normally as if to pick up a glass full of water; unusually fast reaches lack the control needed to adjust trajectory mid-movement. After acquiring and holding still at the target, the subjects were rewarded with an audible tone (humans) and a juice reward (monkeys). Failed trials were punished with a 2s intertrial interval and occasional verbal feedback from the experimenter.

2.3.2.2 Redirect Task

The redirect task was randomly interleaved with the direct task, occurring in 30% or less of the trials. Redirect tasks were identical to the direct reach task except that at an unpredictable time during the movement, a cue indicated that the other target had become the reach goal. This cue could be visual, tactile, or direct microstimulation of the somatosensory cortex. The visual redirect cue was a large blue circle appearing in the center of the screen. (figure 5a). The size of the cue was fairly consistent between human and monkey subjects (about 7-10° of visual angle). Tactile redirect cues were delivered via a vibrating motor placed on the upper arm, back, or hand. The microstimulation redirect cue was a pulse train delivered through an electrode in S1. The duration of all redirect cues was 400ms (figure 5b). The cue modality was randomly interleaved during each session, with 1, 2, or 3 modalities used in a given session. After onset of the redirect cue, the subject was required to reverse reach direction and touch the opposite target to receive their reward (figure 5b); if the hand touched the original reach target before changing direction, the trial would fail immediately.

The response time was quantified as the time between the onset of the redirect cue and the time when the horizontal component of the hand velocity crossed zero (figure 5c). We selected this time as a definitive point in the hand trajectory where it was clear that the stimulus was being acted upon, and could not be mistaken for the deceleration of the reach to the original target. Note that the response time is not a classically-defined "reaction time", which would be harder to measure in this task, but would be strictly shorter. The actual time of onset of the redirect cues were obtained by photo-transistor circuits placed on the monitors, accelerometers fixed to the vibrating motors, and by recording the output of the microstimulator. Lags between the time when

the computer commanded the redirect stimulus and when it actually occurred were 77ms ±14ms (visual), 11ms ±3ms (tactile), and <1ms (microstimulation stimuli).

2.3.2.3 Pressured Reaction Time Task

In monkeys, to elicit the fastest reaction time to a stimulus modality without interference from conflicting motor plans or cognitive demands, we used a delayed center-out task with the stimulus as the go cue. In this "pressured reaction time task", one of eight possible targets appeared, and then after a delay period 300-2500ms (uniformly distributed), a "go" cue appeared. The go cue could be microstimulation, vibrotactile stimulation, or a visual stimulus. In visually cued trials, the start target disappeared. In tactilely cued trials, a small vibrating motor placed on the upper arm turned on until movement began. In microstimulation trials, a 400ms pulse train waveform was delivered through an electrode in S1 to initiate a reach. Ten percent of the trials were "catch trials" in which no go cue appeared, and subjects were rewarded for continuing to hold the start target. Like the direct reach task, the subject's behavior was tightly constrained to penalize early starts and late responses. Early starts were defined as a reach that began prior to 80 ms after the go cue was delivered. At the start of the experiment, the subjects were allowed up to 1500 ms within which they could initiate the reach. That temporal window duration was decreased over the course of each session. Reaction times became faster and less variable as the temporal window tightened. Eventually within the session, the window became so short that the subject could not respond fast enough to succeed in the task. Reaction time was measured as the time from stimulus onset to movement onset. To remove lucky guesses and leisurely responses, the top and bottom 5% of reaction times were removed when calculating the mean. For training purposes we employed the pressured reaction time task without tight time constraints. In this case it is referred to as a stimulus detection task.

2.3.3 Behavioral Timing and Controls

We used a variety of approaches to ensure that our human and monkey subjects made brisk, smooth, and goal-directed reaches. We adjusted task parameters to reduce the prospect of strategies like anticipatory "lucky guessing", hesitations and lingering while awaiting a redirect cue, and early termination of trials. To this end, we distributed the timing of redirect cues so they occurred throughout the reach span. We titrated the trial type distribution, the punish time-out, and the reward volume (for monkeys) to promote smooth performance of the direct reach task. Figure 5c illustrates an example velocity profile. For the redirect task, we noted that the response time was not dependent on the position of the hand along the trajectory.

2.3.4 Tactile Stimulation

Tactile stimuli were delivered via a Jameco Reliapro 1.3V 8500RPM vibrating motor. This device consists of an off-axis asymmetric mass fixed in a plastic capsule. Adjusting the speed of the motor rotation controlled stimulus intensity. For human subjects, the motor was positioned on the back of the non-reaching hand. For monkey subjects the motor was placed on the upper arm of the non-reaching hand, or on the back, to coincide approximately with the receptive field location for the area recorded in S1. The stimulus was set to an intensity sufficient to be readily detected (defined as >95% correct in a simple detection task – the pressured reaction time task described below), but without inducing an overt startle response.

2.3.5 Intracortical Microstimulation

Monkey 2 was implanted with an acrylic-free titanium recording chamber (Adams et al., 2011) placed over intact skull above the somatosensory cortex. A 1 mm burr hole was drilled over the arm area of S1, guided by MRI images. Tactile receptive fields for multineuronal activity ranged from the bicep to the elbow of the non-reaching arm, and remained stable during the course of each session. Neural activity was amplified and played through a loudspeaker; multiunit responses were driven best by brisk brushing of the hair, rather than by constant pressure applied to the receptive field. During most sessions, the depth where neurons were first encountered was noted, then the electrode was advanced an additional 1 to 2 mm during a stimulus detection task until microstimulation was consistently reported. We infer that the 70 penetrations done over the course of our experiments were made into the gyral portion of S1 (area 1), as confirmed by the fact that audible neural activity tapered off when the electrode was advanced by 5 mm or less from where neurons were first encountered without any noticeable change in receptive field. Neurophysiological recording and intracortical microstimulation (ICMS) was accomplished with tungsten electrodes (FHC Inc., Bowdoin, Maine) positioned and manipulated with a Narishige single electrode drive (Narishige Co., LTD, East Meadow, New York).

A computer-controlled pulse generator (A&M Systems, Carlsborg, WA) produced symmetric, biphasic, charge-balanced pulse trains with the cathode phase leading (Koivuniemi & Otto, 2011; Koivuniemi & Otto, 2012). Early in experiments, we designed microstimulation parameters using a range of amplitudes and durations (Katnani & Gandhi, 2012). We used a simple stimulus-detection task in which the animal's "go" cue was microstimulation. We defined threshold as the point at which the stimulation was detected on 93% of trials (figure 6a). This

detection paradigm was briefly recapitulated at the beginning of most sessions. We ascertained that 80 µA was clearly sufficient for detection (figure 6a), and thus used that amplitude in all experiments. Stimulus duration was evaluated in a similar fashion while the amplitude was set at 90µA (figure 6). For all proceeding experiments, duration was set at 400 ms, well within the range of fast responses with high levels of detection (figure 6b). Stimulus frequency was set at 200 Hz (O'Doherty, et al., 2011) and never varied. Pulse widths were 200 µs per phase with 25 µs between phases.

Before and after each training session, stimulus detection was evaluated to ensure peak performance was consistent with that of previous days. Microstimulation was paired with tactile stimulation when it was first introduced to the animal for several sessions, and during most subsequent sessions as a training aid.

We opted to keep the microstimulation site as consistent as possible from one day to the next. Our experiment goal was to measure the fastest reaction times possible under different stimulus modalities. Since monkeys might not generalize as well as humans do, if the stimuli differed from one session to the next, there might be a learning effect as animals learn to use the new stimulus. We wanted to match stimulus conditions for all modalities over days. Thus the visual stimulus conditions were identical, we attempted to put the vibrotactile motors in the same location, and we inserted the electrode into the same burr hole each day.

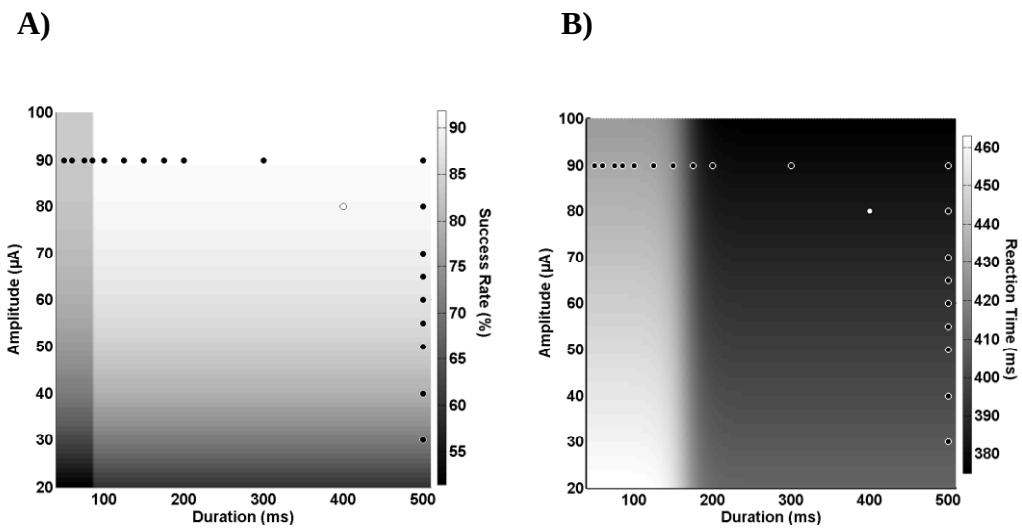

Figure 6. Microstimulation parameters.

(a) Rate of success as a function of stimulus amplitude and duration (b) Reaction time (from stimulus onset to movement onset) as a function of stimulus amplitude and duration. Black dots represent tested stimulus parameters. White dot represents stimulus parameters chosen for the microstimulation redirect cue.

2.4 RESULTS

2.4.1 Human Study

Our main experimental manipulation was a redirect task, in which a cue instructed the subject to alter a reach in mid-flight. The redirect cue could be tactile or visual. We compared the response times to stimuli of different modalities. The response time for tactile stimuli was significantly faster than for visual stimuli across the cohort of ten subjects (Paired t-test $p<0.01$) (figure 7a). The average difference between tactile and visual response times across all subjects was 12ms, with the greatest difference being 23ms, and the smallest being –5ms. For half the subjects,

response times to tactile cues were significantly briefer than for visual cues ($p<0.05$, two-tailed t-test). For the other half, there was a trend toward a faster response to tactile stimuli that did not reach significance, or there was no difference between the two stimulus types (figure 7a). We found no subjects for whom the response to a visual cue was significantly faster than the response to a tactile cue.

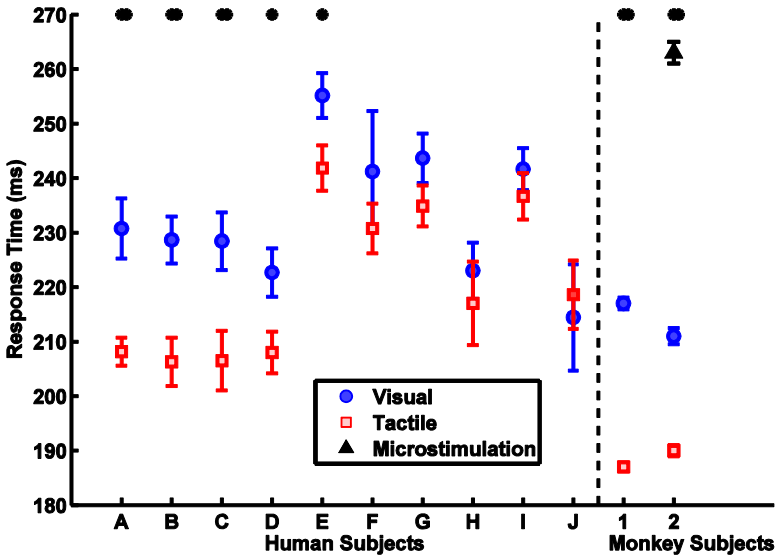

Figure 7. Response time depends on stimulus modality.

(a) Mean human and monkey (right of dashed line) response times to visual cues (solid blue circle), tactile cues (hollow red square), and for monkey 2, microstimulation cues (solid black triangle). Bars indicate standard error. *: $p<0.05$; **: $p<0.01$ pairwise comparison for all modalities

A)

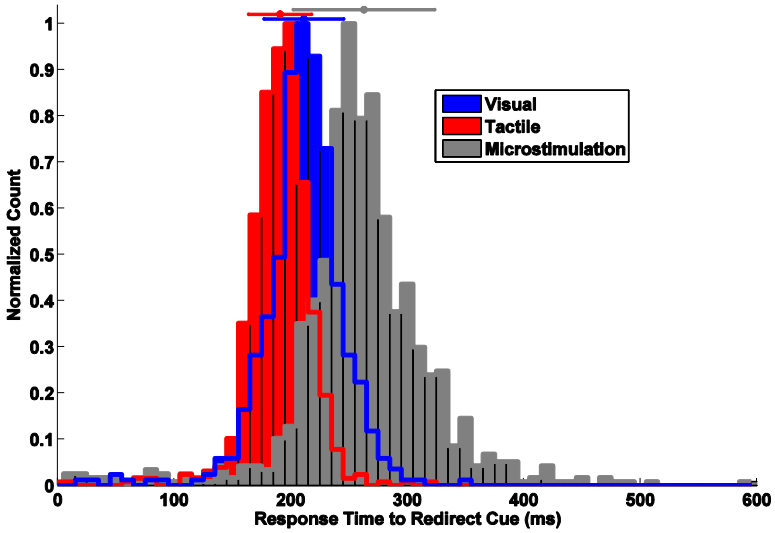

B)

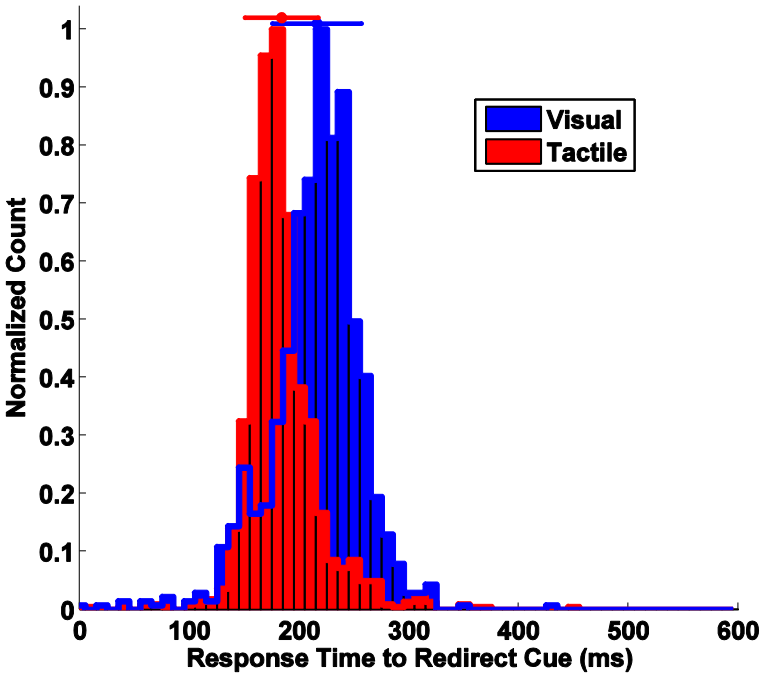

Figure 8. Monkey response time depends on stimulus modality.

(a) Monkey 2 response time histogram for visual (blue), tactile (red), and microstimulation (gray) redirect cues. (b) Monkey 1 response time histogram for visual (blue) and tactile (red) redirect cues.

2.4.2 Monkey Study

2.4.2.1 Visual and Tactile Redirect Task

The redirect task with visual and tactile cues was conducted with two Rhesus monkey subjects. Both animals were over-trained on the tasks and produced movements with a bell-shaped velocity profile (Morasso, 1981) (figure 5c). Pooling data across multiple sessions (Monkey 1=24, Monkey 2= 31), the mean response time for tactile cues was faster than for visual cues (188 ms versus 217 ms for monkey 1; 190 ms vs 211 ms for monkey 2, $p < 0.001$, t-test) (figure 7 & 8). Tactile response times were also significantly faster in every individual session (figure 9). This difference in response times for the two modalities (21 and 29ms) is approximately as large as the largest difference in response times observed among the human subjects (23ms).

The vibrating motors are audible. To control for the possibility the animals responded to the audio cues, we placed the stimulator on the rig beside monkey 2 so he could not feel it. After a brief training block, the monkey did respond to the sound of the stimulator, but the mean response time was 230 +/- 20ms, slower than for both the tactile and the visual redirect cues.

2.4.2.2 Microstimulation Redirect Task

We found that tactile cues can be used to influence behavior more rapidly than visual cues can. This makes sense based on the latency of neural responses in primary sensory cortices: 30-50ms for primary visual cortex (Maunsell JH & Gibson JR, 1992) and ~15 ms for S1 (Sripati AP, et al., 2006). The bulk of that processing delay is in sensory transduction. We reasoned that response times would be even faster if a signal were provided directly to the brain, since it would bypass afferent pathways.

We tested this hypothesis by using microstimulation in S1 as the redirect cue. We predicted response times would be faster than for tactile stimuli by about 15ms. After becoming proficient at the redirect task, monkey 2 was implanted with a recording chamber and given microstimulation via a single electrode. We stimulated within area 1 of the somatosensory cortex (S1) in the vicinity of quickly adapting neurons. When microstimulation was first introduced, it was trained in combination with the tactile cue for stimulus detection tasks and then redirect tasks. The animal began to make the association within the first day and became proficient at using only microstimulation after two weeks of daily training. Across 23 sessions, response times for microstimulation cues were significantly slower than for tactile redirect cues (263 vs 190 ms, $p < 0.001$) and even visual redirect cues (263 vs 211 ms) (figure 8a).

We considered whether extended experience with microstimulation might improve its latency. There was a decrease in latency over the first two weeks while the animal learned the task, but after becoming proficient (>80% correct for early redirect cues) no further improvements were noted. The difference in response time between modalities was in the same order and significantly different in each pairwise comparison for each day (figure 9a).

A)

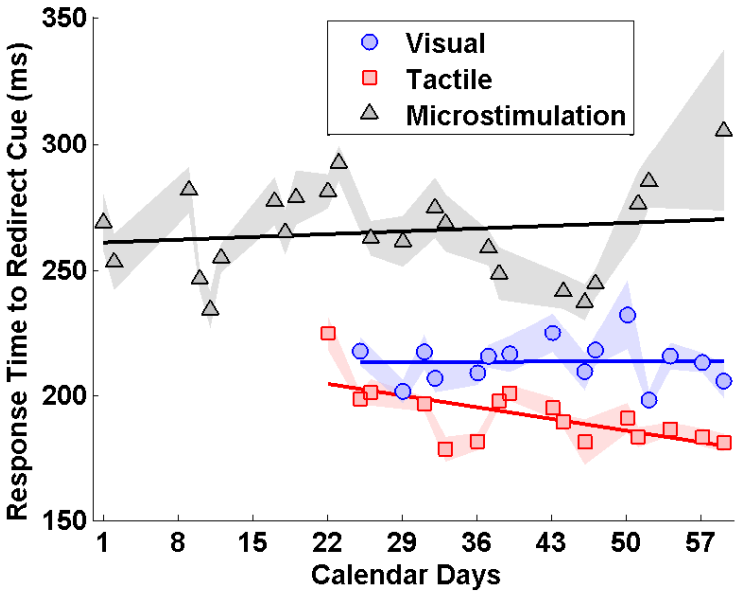

B)

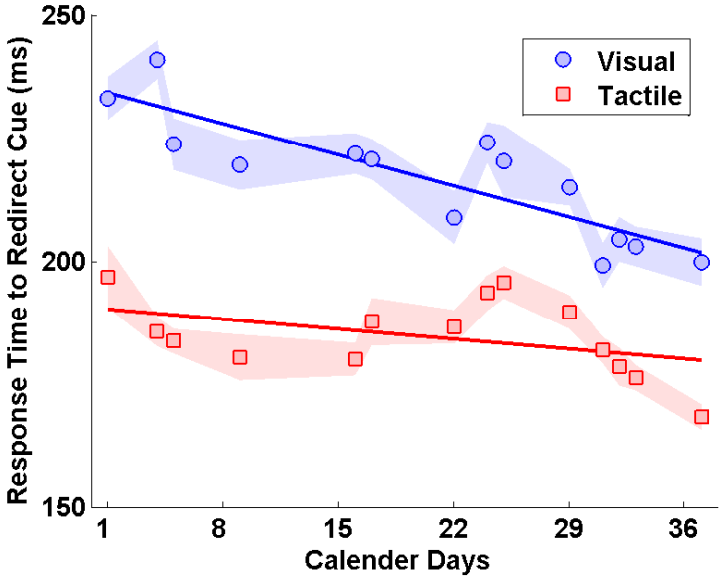

Figure 9. Response time across days.

(a) Mean reaction times and standard error for monkey 2 plotted across days with regression line for visual, tactile, and microstimulation redirect cues. Regression line slopes are not significantly different from zero. (b) Mean reaction times and standard error for monkey 1. Visual regression line slope is significantly different from zero. ($p<0.01$) Tactile regression line is not significant ($p=0.12$)

2.4.2.3 Critical Feedback Point

If feedback is too slow, it cannot influence behavior. Another way to express the feasibility of a feedback modality is to identify a spatial critical feedback point beyond which the feedback arrives too late to alter a movement. For better (i.e. faster) feedback modalities, this critical feedback point occurs later in the movement. Success at responding to the redirect cue decreases to zero the closer the subject's hand gets to the target. Figure 10 shows performance as a function of the hand position at the time the redirect cue is given for monkey 2. We define the critical feedback point as the position along the reach trajectory beyond which the animal has a <50% chance of successfully responding to the redirect cue. The critical feedback point for tactile and visual cues is at 37 and 38.5mm from the target, while for microstimulation, the critical is at 60mm from the target. Thus tactile and visual cues could provide actionable information until much later in the movement than could microstimulation cues.

Figure 10 also makes evident that even when delivered sufficiently early in the reach, microstimulation cues were considerably less reliable than visual or tactile cues in eliciting a redirected reach (~80% percent correct in responding to a microstimulation cue presented just after the reach begins, versus ~90% for visual and tactile). Note that this difference in ideal performance does not account for the differences in the critical feedback point. Even if the baseline performance had matched the other modalities, the critical feedback point would have occurred earlier in the reach for microstimulation (55mm from the target)

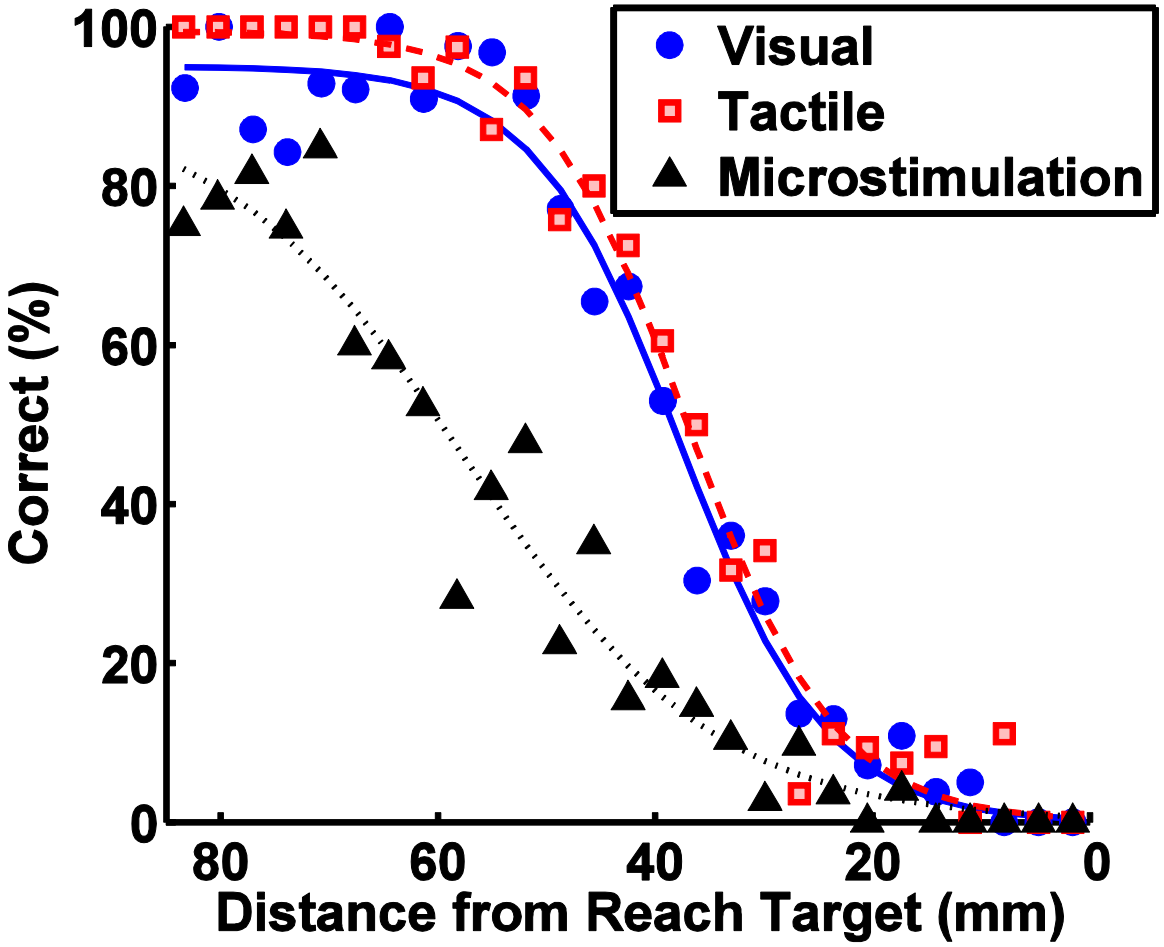

Figure 10. Likelihood of success based on hand position at the time the redirect cue is given. Success Rates for binned trials every 3 mm. Lines are best logistic fit for visual (R2=0.98), tactile (R2=0.99), and microstimulation (R2=0.95) cued trials. The start target window extended to 83mm from the reach target.

2.4.2.4 Pressured Reaction Time Task

The response to microstimulation during an ongoing movement was slower than we predicted. Cognitive demands of the redirect task might impair the animal's ability to respond to microstimulation. We simplified the task in order to measure very directly how rapidly microstimulation could be used to influence behavior. In this task, the pressured reaction time task,

the monkey was required to react as quickly as possible to a cue. A visual, tactile, or microstimulation stimulus served as the "go" cue in a delayed center-out reaching paradigm. This allowed us to measure reaction times to the stimulus without interference of conflicting motor plans or sensory feedback. Still, the animal's response to microstimulation was slower than the response to tactile and visual cues (**table** 1).

Table 1. Reaction times in the pressured reaction time task and response times in the redirect task

Modality	Response Time (ms)	Reaction Time (ms)
Visual	211 +/- 34	222 +/- 48
Tactile	190 +/- 27	184 +/- 41
Microstimulation	263 +/- 60	237 +/- 34

2.5 DISCUSSION

A crucial direction in the improvement of brain-computer interface performance is to provide fast, salient, informative feedback signals to BCI users (Weber, et al., 2012). In this study we compared the feasibility of three sensory modalities (vision, touch, and somatosensory microstimulation) as potential feedback signals to influence an ongoing movement. We defined a fundamental element of feedback as the ability of subjects to quickly adjust an ongoing movement once they were provided with new sensory information about their movement goal. While human and monkey subjects reached toward visible targets, cues were presented that indicated a change in the goal location. Our first main finding is that tactile cues could be utilized to change the ongoing reach more rapidly than could visual cues. This suggests that a tactile feedback-based BCI could enhance BCI performance, at least in temporal aspects, compared to devices that provide only visual

feedback. Of course, the tactile feedback would need to be provided on a body part not affected by the impairment. Our results indicate that such sensory transfer will not be a problem – our tactile stimulator was placed on the limb opposite to the reaching arm, and was behaviorally efficacious.

We did not attempt to mimic the natural sensory experience that would arise during a reach. Instead we focused on the question of whether an abstract sensory signal can provide meaningful feedback. Several considerations motivated this design choice. First, in a BCI context, for a patient with sensory loss as well as motor impairment, mimicking the natural sensory experience is a prospect that will face many challenges (Weber, et al., 2012). Second, the visual stimulus was a large central flash of light – which does not resemble naturally occurring feedback – and we opted to compare tactile and visual stimuli as directly as we could.

Response times to tactile and visual cues have been compared in other studies, for example (Forster, et al., 2002; Diederich & Colonius, 2004), but in prior work the stimuli were used to indicate movement initiation, not to alter an ongoing movement. To our knowledge this is the first demonstration that tactile information can be used more rapidly than visual information to alter an ongoing movement. Considering that an ongoing movement can alter afferent sensory responses (Graziano MS, et al., 2002), this was important to verify. It is also important to have this information in a substantial cohort of subjects (n=10). It is clear that the feedback modality should be customized for each subject.

Our second main finding is that microstimulation can also serve as an informative stimulus modality to alter an ongoing movement. Microstimulation in sensory cortical areas has a long and impressive history as a means of providing sensory information to the brain (Salzman CD, et al., 1990 ; Romo, et al., 1998; Berg, et al., 2013). Microstimulation in motor areas rapidly causes a

movement (Fritsch & Hitzig, 1870; Schiller PH & Sandell, 1983; Bruce, et al., 1985). We reasoned that microstimulation in sensory areas could be used to adjust an ongoing movement more rapidly than tactile stimulation, since microstimulation can bypass sensory transduction delays. We were surprised to discover that microstimulation affected behavior considerably more slowly than did tactile and visual stimuli. To verify this observation we delivered sensory cues in a pared-down paradigm in which the animal simply had to react rapidly to the cue. Behavioral responses to microstimulation were still 53ms slower than to tactile stimulation.

2.5.1 Why is Microstimulation Feedback so slow?

Our results indicate that the neural activity induced by electrical stimulation must undergo further neural processing before it can influence behavior. Why might further processing be necessary? First, it may be that amplification by downstream processing is needed. If microstimulation were applied at an earlier stage in the sensory processing hierarchy, it might harness cortical circuitry to become amplified into a behaviorally meaningful signal. The somatosensory portion of the thalamus (the core of the ventral posterior lateral region) projects to areas 1, 2, 3a, and 3b, with the strongest projection going to 3b. Had we stimulated in the thalamus or in an "earlier" cortical recipient zone, the response to microstimulation might have been faster. Second, it might be that further processing is needed to refine microstimulation into a usable signal. Microstimulation presumably activates excitatory and inhibitory cell bodies, as well as fibers of passage (Butovas & Schwarz, 2003). There may be a local competition among these processing units before cortical activity patterns can settle into "natural" patterns capable of influencing behavior. In support of the role of further cortical processing in amplifying and refining artificial signals, Horwitz and colleagues (Jazayeri, et al., 2012) elicited a behavioral response with optogenetic stimulation in

primary visual cortex. They speculated that these effects might not have occurred if they had stimulated downstream, thereby bypassing the amplification provided by subsequent cortical processing.

However, these explanations do not seem adequate to explain all the phenomena. In our tasks the animals only had to use the presence of a stimulus to react; they were not required to interpret it in any naturalistic manner. Stimulus detection is known to be a faster process than stimulus discrimination (VanDerLubbe, et al., 2001). Also, when peripheral nerves are stimulated in humans, they report that the sensation feels "artificial" (Daly, et al., 2012)

2.5.2 Perceptual Comparisons

Many authors have shown behavioral effects of stimulating in sensory areas, including (Romo, et al., 1998; Romo, et al., 2000; Romo, et al., 2002; Liu & Newsome, 2000; Ohara, et al., 2004; Koivuniemi & Otto, 2012; Tehovnik & Slocum, 2005). A question that underlies all these studies, not directly addressable using non-human subjects, is what perceptions are evoked by microstimulation in sensory areas? If the evoked perception from microstimulating S1 were similar to those evoked by stimulating the skin with tactile stimuli, then after a task is learned for tactile cues, replacing those cues with microstimulation should produce only marginal drops in performance and engender a rapid understanding of the new stimulus. In studies stimulating area 3b, monkeys were able to compare the frequency of a microstimulation stimulus to a tactile stimulus (Romo, et al., 2000). Additionally, this comparison task was trained in only a few days, presumably because somatosensory microstimulation "felt like" touch to the animals. In contrast, other authors stimulating in area 1 have reported extensive training was required for animals to affiliate microstimulation with touch (Fitzsimmons, et al., 2007).

When stimulating in area 1, we verified that extensive training is required. When the microstimulation was first introduced, the animal ignored it until it was paired with a natural stimulus. We first paired microstimulation and tactile stimuli using our detection task. Once the animal could react to microstimulation alone reliably in that simple task, we introduced microstimulation alone in the redirect task. Again, the animal would not react to the microstimulation until it was paired with tactile stimuli in the redirect task. After this new role for microstimulation had been learned, it was remembered in subsequent days of training without pairing. The perceptions for the two stimuli, microstimulation and tactile, were different enough that no perception-based association was made in either task. Only when the cues occurred simultaneously, with a direct side-by-side comparison, could the association then be made.

2.5.3 Applications to BCI

Our goal was to inform the design of feedback for BCIs. To provide feedback usable to guide an ongoing movement, a sensory modality should be informative and fast. Most current BCIs function solely under visual feedback. While vision is highly informative, it is slow. Our data suggest that a tactile-based feedback scheme might complement visual feedback by providing faster information. To our surprise, microstimulation-based feedback, at least in area 1, affected behavior more slowly than did tactile and visual feedback. We targeted area 1 for this study, since it is on the cortical surface, and thus is the most accessible target for a flat multielectrode array (Blackrock Systems Inc.). It may be that carefully designed patterns of microstimulation across a multielectrode implant (O'Doherty, et al., 2009) might provide richer, faster feedback than we could achieve with a single electrode. Microstimulation patterning might be designed to mimic the responses that are recorded during actual touch (Weber, et al., 2012).

Our study provides a strategy for the quantification of the effectiveness of temporal aspects of sensory feedback. It also highlights the need of careful quantifications like these; it cannot simply be assumed that microstimulation will yield a superior form of feedback in comparison to simpler approaches such as tactile and visual stimulation.

3.0 DIRECTION AND SPEED TUNING OF MOTOR-CORTEX MULTI-UNIT ACTIVITY AND LOCAL FIELD POTENTIALS DURING REACHING MOVEMENTS

3.1 ABSTRACT

Primary motor-cortex multi-unit activity (MUA) and local-field potentials (LFPs) have both been suggested as potential control signals for brain-computer interfaces (BCIs) aimed at movement restoration. Some studies report that LFP- based decoding is comparable to spiking-based decoding, while others offer contradicting evidence. Differences in experimental paradigms, tuning models and decoding techniques make it hard to directly compare these results. Here, we use regression and mutual information analyses to study how MUA and LFP encode various kinematic parameters during reaching movements. We find that in addition to previously reported directional tuning, MUA also contains prominent speed tuning. LFP activity in low-frequency bands (15-40Hz, LFP_L) is primarily speed tuned, and contains more speed information than both high-frequency LFP (100-300Hz, LFP_H) and MUA. LFP_H contains more directional information compared to LFP_L, but less information when compared with MUA. Our results suggest that a velocity and speed-encoding model is most appropriate for both MUA and LFP_H, whereas a speed only encoding model is adequate for LFP_L.

3.2 INTRODUCTION

Primary motor-cortex (M1) is the major area for harnessing neural signals for brain-computer interface (BCI) control. In recent years, single-unit activity (SUA), multi-unit activity (MUA) and local-field potentials (LFPs) have been proposed as possible control signals for BCIs. While the relationship of SUA to various movement parameters during reaching movements has been extensively studied (Georgopoulos, et al., 1982; Flament & Hore, 1988; Fu, et al., 1995; Scott, et al., 1997; Moran & Schwartz, 1999; Paninski, 2004; Paninski, et al., 2004), that of MUA and LFP is not as well understood. Several groups have studied low-frequency LFP in the time or frequency domain, concluding that it encodes hand position, direction or velocity information (Mehring, et al., 2003; Rickert, et al., 2005; Asher, et al., 2007; Stark & Abeles, 2007; Bansal, et al., 2011; Liu & Newsome, 2006). Studies of high-frequency LFP in the frequency-domain have shown similar results (Rickert, et al., 2005; Liu & Newsome, 2006; Heldman, et al., 2006; Zhuang, et al., 2010; Zhuang, et al., 2010 ; Flint, et al., 2012; Bansal, et al., 2012). Comparisons of movement related information encoded by LFP to that encoded by either SUA or MUA have resulted in contradicting results: some studies have reported that the amount of information encoded by LFP exceeds that encoded by spiking activity, while other studies report less movement related information in LFP than in spiking.

Several factors could account for this discrepancy. First, experimental paradigms differ across the various groups. Second, while some studies used averaged neural activity, others used instantaneous activity. Third, some studies decoded kinematics from neural activity, while others used mutual-information (MI) or linear correlation based analyses. Finally, each of the studies made different assumptions about the encoding model.

Here, we extend previous work by systematically studying tuning properties of LFP and comparing them to MUA tuning. Motor-cortical SUA has been previously shown to encode both direction and speed (Moran & Schwartz, 1999). We therefore considered tuning models which included direction, velocity, speed and their additive combinations. We used instantaneous neural activity and kinematics, as opposed to averaged data, to make our conclusions more relevant for real-time BCI use. We found that MUA exhibited prominent speed tuning, along with directional tuning which was especially evident in a small subset of the channels examined. Low- and high-frequency LFP were speed tuned. Some high-frequency LFP channels demonstrated directional tuning similar to that of MUA.

3.3 METHODS

3.3.1 Behavioral Task and Data Collection

A Rhesus monkey was trained to perform center-out movements using the arm contralateral to the recording site. The animal was comfortably seated in a primate chair, in front of a computer screen, with one arm restrained and the other free to move behind the screen, thus obscured from the animal. An active marker system (Phasespace Inc, San Leandro, CA) was used to track its hand position in real- time. This 3D position was projected to a 2D plane and was used to render a cursor on the computer screen in real-time. At the beginning of each trial, a center target appeared and the animal had to move its hand so that the cursor location matched the center target. Then, after 200-400ms, a peripheral target appeared. The animal reached so the cursor moved to the peripheral target, within ~800ms, or else the trial would fail. Successful trials were indicated with a water

reward. On some trials, the animal had to move its hand so the cursor followed paths of varying shapes and thicknesses. On most trials, the hand path was not constrained. Neural tuning did not seem to differ between these two tasks, so those data were combined for the analyses described here.

After the animal had sufficient proficiency in the task, a 96-electrode silicon array (Blackrock Systems Inc.) was chronically implanted in the arm region of the contralateral motor-cortex. All surgical procedures followed protocols approved by the University of Pittsburgh Institutional Animal Care and Use Committee. Post-surgery, the animal resumed performing the task while neural activity was recorded and stored for off-line analysis using a TDT system (Tucker-Davis Technologies, Florida). The 3D hand position (sampled at 120Hz) and relevant task information were stored in synchronization with the neural data.

An RMS based threshold was used to obtain threshold-crossing event times for every channel. Here, we refer to these threshold-crossing events as MUA, but that does not necessarily imply these are multi-unit clusters of neural activity that are well separated from the noise floor. LFP activity was obtained by band-pass filtering channel voltage signals (10-500Hz), and was stored at a sampling rate of 1220Hz. Off-line, MUA threshold-crossings were converted to firing-rates by counting events in consecutive 100ms bins and dividing by the bin width. The LFP power-spectral density (PSD) was computed at a temporal resolution of 16ms with a frequency resolution of 5Hz using the mem library (BCI2000 Project [19]), and then log-transformed. In the analyses presented in this paper, we used two frequency-bands: 15-40Hz (LFP_L) and 100-300Hz (LFP_H). These two bands demonstrate the two major types of modulation commonly found in LFP during reaching movements (suppression and facilitation relative to baseline, e.g. (Mollazadeh, et al., 2011). Due to noise artifacts in the frequency band 28-32Hz, these frequencies were notch-filtered

prior to computing the LFP PSD. We chose the LFP_L and LFP_H frequency bands based on both single channel and channel averaged normalized time frequency plots. We found that frequencies in these ranges tended to demonstrate similar tuning (data not shown). Furthermore, R^2 values for the 41-99Hz band (see sec. II-B) were significantly lower compared to the other two bands; hence we ignored it in further analyses.

3.3.2 Tuning Models Estimation

Based on previous studies, suggesting that SUA contains both directional and speed information (Moran & Schwartz, 1999), we considered the following 5 tuning models:

$$y = b_0 + b_x d_x + b_y d_y + noise \quad (1)$$

$$y = b_0 + b_x v_x + b_y v_y + noise \quad (2)$$

$$y = b_0 + b_s s + noise \quad (3)$$

$$y = b_0 + b_x d_x + b_y d_y + b_s s + noise \quad (4)$$

$$y = b_0 + b_x v_x + b_y v_y + b_s s + noise \quad (5)$$

where:

- y is a single-channel MUA instantaneous firing-rate in Hz, or a single channel log-transformed instantaneous LFP PSD averaged across a given frequency band
- $\vec{d} = (d_x, d_y) = (\cos\theta, \sin\theta)$ is the instantaneous direction of hand movement
- $\vec{v}$ is the instantaneous hand velocity
- $s = |\vec{v}|$ is the instantaneous hand speed

These models relate neural activity to instantaneous direction (eq. 1), velocity (eq. 2), speed (eq. 3), direction & speed (eq. 4), and velocity & speed (eq. 5). Together, they allow systematic

investigation of how MUA and LFP relate to direction and speed components in a multiplicative or additive manner. Prior to fitting the regression models, MUA firing-rate and kinematic features were spline-interpolated to match the LFP PSD sampling frequency. We also performed a lag analysis, where we fit the above models with varying lags between the neural and kinematic features. We considered lags ranging from causal values (-300ms) to non-causal values (+400ms), at 50ms steps. For most MUA channels, the best fits, as determined by coefficient of determination (R^2) values, were obtained with causal lags in the range of -100 to -150ms. For real-time BCI control, a single time-lag would likely be used for all channels; therefore we chose a causal lag of 100ms for all channels (MUA and LFP), for all analyses in this paper.

3.3.3 Mutual Information Estimation

The models in eq. 1-5 explore the linear relationship between neural activity (MUA, LFP) and velocity, direction and/or speed. However, if neural activity is linearly related to velocity, then it might be non-linearly related to its magnitude (speed). We therefore explored non-linear relationships between neural and kinematic features, in the form of mutual- information (MI), which measures any dependency between two random variables, regardless of its functional form. MI was empirically estimated by:

$$MI(X;Y) = \sum_{x\in X}\sum_{y\in Y} p(x,y)\log\frac{p(x,y)}{p(x)p(y)} \qquad (6)$$

where:

- Y represents single-channel instantaneous neural activity
- X represents instantaneous direction or speed

Empirical MI estimations are sensitive to data discretization; hence we chose the following discretization schemes. Given that the behavioral task used peripheral targets at roughly 8 regions around the center target, we discretized movement direction (θ) to 8 bins. To ensure similar entropy for direction and speed, speed was discretized to 8 bins as well. We used varying bin widths resulting in close to uniform marginal distributions for direction and speed. For Y, we used MUA spike counts in 100ms bins, or discretized LFP PSD for a given frequency-band.

Empirical MI estimates tend to be positively biased (Treves & Panzeri, 1995). We estimated this bias by permuting the neural data and computing the MI to direction and speed 100 times; then computing the bias as the mean of these 100 null MI values. This bias estimate was then subtracted from the MI estimate, for every channel and neural data type, in all the analyses described here.

To determine an optimal discretization for LFP PSD, we computed the bias-corrected MI using 5-305 bins (in steps of 5). As expected, both the MI and bias increased with the number of bins, but bias-corrected MI estimates for all LFP channels and frequency bands tended to plateau for more than 25 bins. We therefore discretized LFP PSD using 25 bins.

3.4 RESULTS

3.4.1 Linear Tuning to Kinematics

We first explored linear tuning of MUA and LFP to direction, velocity and speed using the regression models from sec. II-B. We fit the models using data from multiple recording sessions and results were qualitatively similar. We chose to present data from the two sessions with the

largest number of trials. Figure 11 summarizes our findings in the form of R^2 box-plots across all channels, one for every model and neural modality (MUA, LFP_L, LFP_H). It should be noted that R^2 values are lower than those previously reported using averaged data, because we used instantaneous non-smoothed data, as would be the case in on-line BCI control.

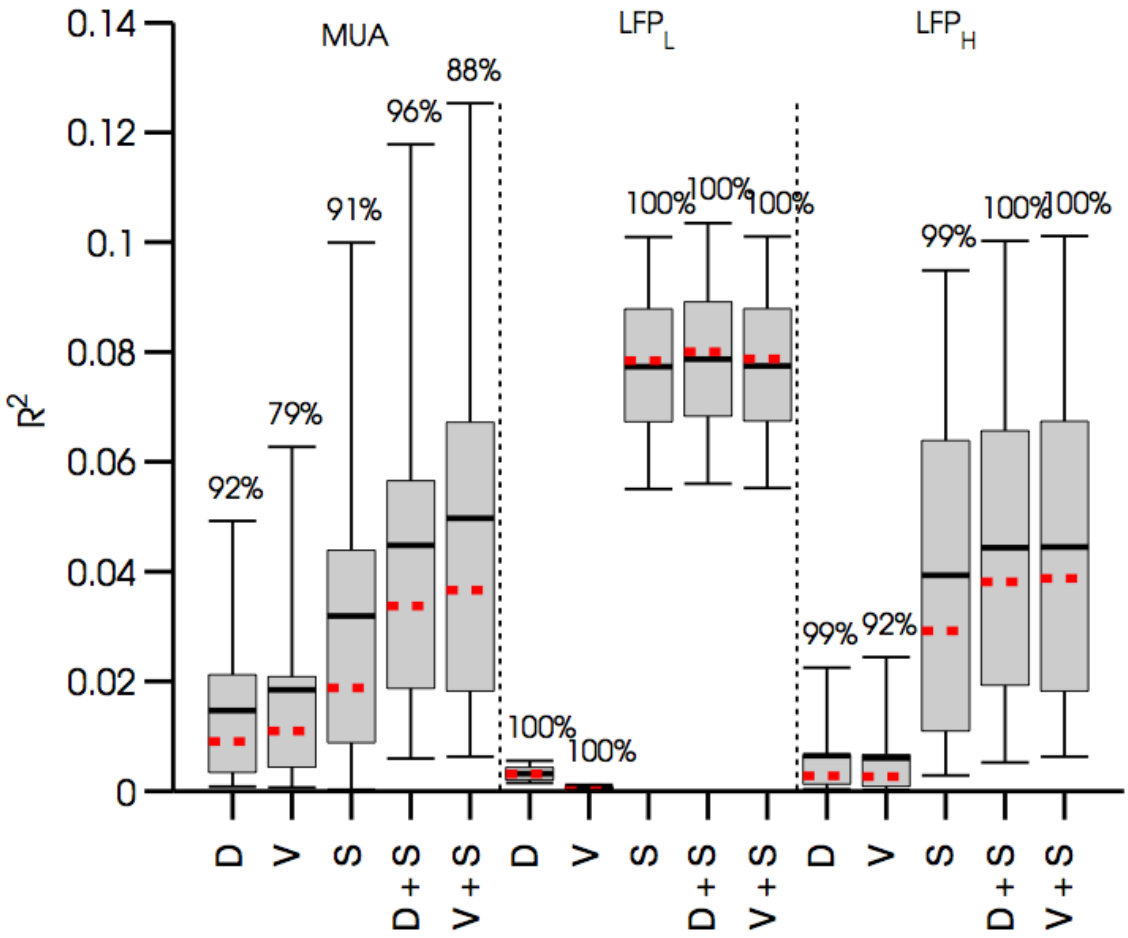

Figure 11. MUA and LFP tuning model R^2.

Population tuning model R2 for the 5 models described in sec. 3.3.2: Direction (D), Velocity (V), Speed (S), Direction & Speed (D+S), Velocity & Speed (V+S). Box-plots describe the 5th, 25th,75th and 95th R^2 percentiles, as well as the mean (solid line) and median (dashed line) R^2, across all channels with significant regressions. Percentages above the 95th percentile indicate the proportion of significant regressions among 87 channels. MUA demonstrates the strongest direction and velocity tuning. MUA speed tuning is prominent. Most LFP_L and LFP_H channels are speed tuned. Some LFP_H channels show direction and velocity tuning, equivalent to MUA. LFP_L shows the strongest speed tuning across the three modalities.

While previously published results indicated that SUA encodes direction or velocity (Moran & Schwartz, 1999; Stark & Abeles, 2007; Flint, et al., 2012), we found that MUA encoded speed better than either direction or velocity, possibly due to the fact that threshold-crossing events in MUA originated from multiple single-units with different directional tuning. The two models incorporating direction & speed (eq. 4) or velocity & speed (eq. 5) yielded the highest R^2 values across MUA channels. These models were better than either speed, direction, or velocity only models, indicating that MUA encoded directional information which was independent of speed information. The differences between the mean and median R^2 for all models indicated that the R^2 distribution has a long positive tail. Therefore, MUA tuning was heterogeneous, where a small subset of channels (~20%) encoded the kinematic features better than the other channels.

We found that LFP_L encoded only speed, with no evidence of directional tuning. The difference between the LFP_L mean and median R^2 was very small, suggesting that LFP_L speed tuning was homogeneous, in the sense that most channels encoded speed equally well. Most LFP_H channels contained prominent speed tuning, but in contrast to LFP_L, a subset of channels (~20%) were also directionally tuned.

Figure 11 also allows us to compare tuning across neural modalities. As expected, most MUA channels encoded direction and velocity better than either LFP_L or LFP_H channels. A subset of LFP_H channels (~20%) demonstrated direction or velocity R^2 values equivalent to the average MUA R^2. Speed was best encoded by LFP_L: the worst LFP_L channels encoded speed better than ~80% of MUA channels and ~70% of LFP_H channels.

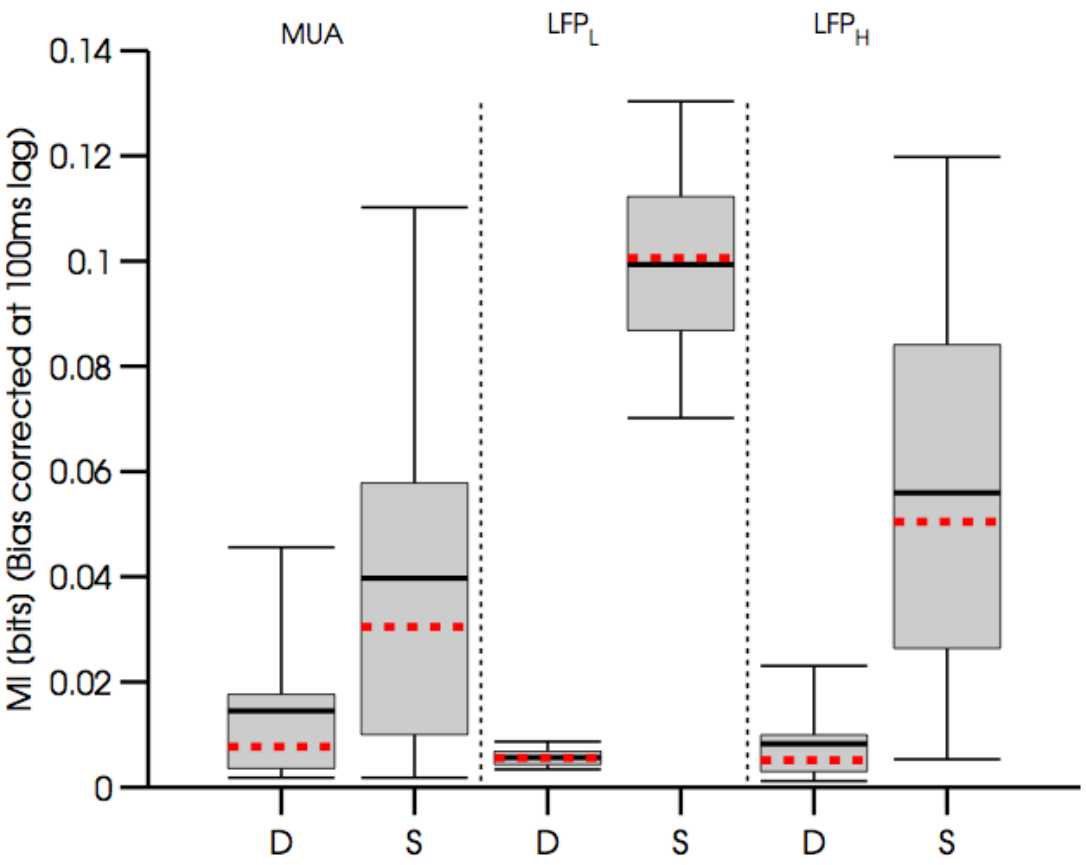

Figure 12. MUA and LFP MI comparison.

MI between MUA, LFPL, LFPH and kinematics (direction and speed) is compared. MI between MUA and direction is the highest among the three modalities. MI between LFPL and speed is the highest among the three modalities. Compare to figure 11 where linear tuning is shown.

3.4.2 Non-linear Tuning to Kinematics

We used the information theoretic analysis described in sec. II-C to capture potential non-linear dependencies between MUA, LFP_L, LFP_H and direction or speed, beyond the linear tuning described in sec. III-A. Figure 12 shows box-plots of MI values across all channels and neural modalities. The results in figure 12 are qualitatively similar to figure 11. Direction was best encoded by MUA, followed by a subset of LFP_H channels with weaker direction encoding. While

MI(LFP_L;*direction*) was very low, MI(LFP_L;*speed*) was higher than MI(*MUA;direction*). MI(*MUA;speed*) and MI(LFP_H;*speed*) were similar across channels, both lower than MI(LFP_L;*speed*). These results support the tuning analyses in sec. 3.4.1, suggesting that linear models adequately describe the relationships between MUA, LFP and speed or direction.

3.5 DISCUSSION

Multi-unit activity (MUA) and local-field potentials (LFPs) are two potential control signals for brain-computer interfaces. Recent studies relating MUA and LFP to various movement kinematics resulted in disagreement. Some studies suggest that LFP based decoding is equivalent to MUA based decoding, while other studies have found MUA based decoding to be superior. One possible reason for the contradicting results is the different tuning models used in those studies. Another reason could be data pre-processing: some studies used averaged data, others applied different filters to instantaneous data. The relative time-lags between neural data and kinematics also varied across studies.

Here, we studied a rich set of MUA and LFP encoding models using instantaneous non-filtered data, with a fixed lag, to closely match the type of data used in on-line BCI studies. We found that while MUA was directionally tuned, as previously reported, it was more strongly tuned to speed. Based on this finding, decoding models utilizing MUA would benefit from taking speed tuning into account. A velocity-speed encoding model (eq. 5) best represented MUA tuning in our data. MUA tuning was heterogeneous across channels: some channels encoded speed or direction much better than others. This suggests that BCI decoding might also benefit from some form of channel selection criteria.

Of the models we tested, we found that our low-frequency LFP activity (LFP_L) was driven predominantly by speed, and that LFP_L activity across channels was highly correlated. High-frequency LFP activity (LFP_H) encoded both speed and direction, although directional information was lower compared to MUA. LFP_H activity across electrodes was more heterogeneous compared to LFP_L: similarly to MUA, a subset of LFP_H channels best encoded speed or direction. We determined that the most appropriate LFP_L encoding model was a speed only model (eq. 3), whereas a velocity-speed encoding model (eq. 5) best described LFP_H tuning.

Our regression and mutual-information analyses showed similar trends for both MUA and LFP, suggesting that linear direction and speed models adequately capture the neural tuning in our data. Based on our findings, a hybrid MUA-LFP decoder, accounting for the prominent speed tuning in both neural modalities, should prove superior to velocity-only based decoders.

4.0 ACHIEVING PRECISE TEMPORAL CONTROL FOR TIME-CRITICAL EXPERIMENTS

4.1 STATEMENT OF PURPOSE

The experiments preformed in chapter 2 dealt with the precise timing of stimulus onset and the resulting behavioral response. The response and reaction times observed were below 500ms with significant behavioral differences between the stimuli being as small as 20ms. If the stimulus onset had any unmonitored temporal delays larger than 1ms, it could have a dramatic effect on the results obtained, not only artificially inflating the standard deviation, but also shifting the perceived mean response time for that one stimulus while not affecting another, thus changing the perceived difference in behavioral response all together. For instance, typical LCD monitors have a refresh rate of 60Hz, so a lag of 1-16ms can be expected depending on where in the display cycle the command to change the visual stimulus is given. This does not take into account any lags associated with rendering the new graphics. The purpose of this chapter is to explain how to account for and remove the following lags from data:

- Graphics computer delay and monitor refresh via photodetector
- Motor ramp-up time via accelerometer
- Microstimulation stimulus onset delay via oscilloscope readout
- Phasespace-to-Host-to-RT lag via internal sync signal

Due to the close proximity of some of these monitoring devices to the subjects and the fragile nature of the equipment, general maintenance notes are also provided. All matlab functions mentioned by name are located on the accompanying flash-drive.

4.2 VISUAL DISPLAY ONSET SYNCED BY PHOTODETECTOR

The LCD monitors in the behavioral rig have a refresh rate of 60Hz, meaning it will take 1-16ms to display each instructed display change. This does not take into account any lags associated with rendering the new graphics. We used a phototransistor circuit to monitor precisely when these visual changes occurred so that the time of visual presentation could be synced with the Real-Time machine's internal clock.

4.2.1 Phototransistor Circuit

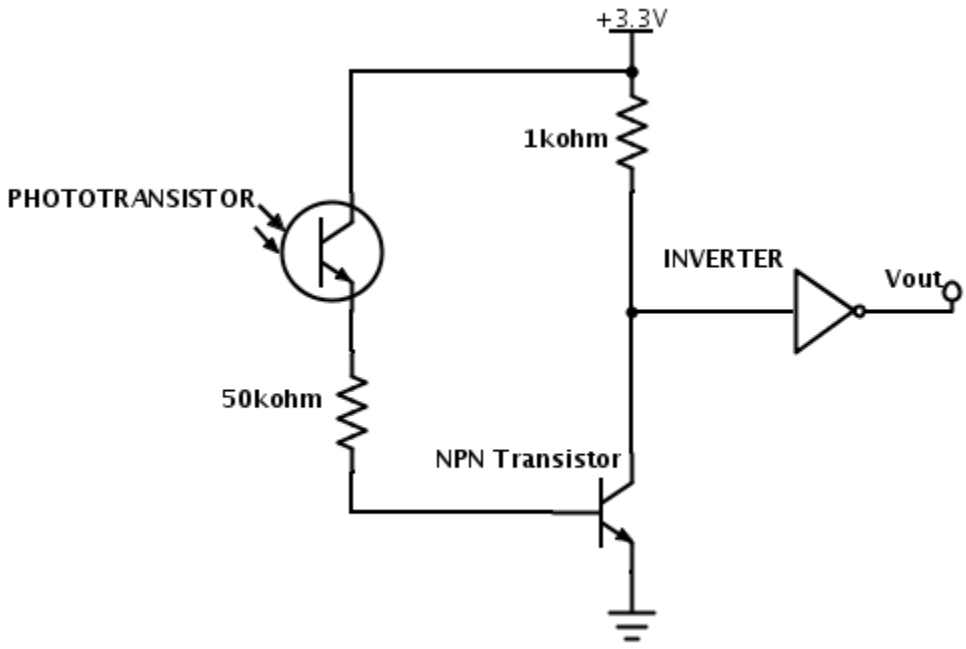

Figure 13. Phototransistor circuit diagram.

Component list:

- Phototransistor: PNZ102-ND
- Transistor: 2N3904

- Inverter/NOT gate: 7404
- Resistors: 1kΩ & 50kΩ
- 3.3V AC/DC Adapter

The circuit box is placed near the monitor with the phototransistor fixed directly on the monitor screen. The receptive frequency of the phototransistor should be chosen so that it responds to the visual wavelength of the monitor and becomes open when placed over a white area of the screen and closed when placed over a black area of the screen. When no light is present, the circuit in figure 13 allows current to flow freely towards the voltage out port (V_{OUT}), which is connected to the Host DAQ card. An inverter was placed between the current source and V_{OUT} to invert that voltage to 0 volts. When light shines on the phototransistor, the input to the inverter to V_{OUT} becomes grounded, which inverted, makes V_{OUT} go to 3.3V. The inverter was used in this circuit to stabilize the signal, making it a clear step in voltage and also to make 0 volts represent darkness and 3.3V represent the presence of light to avoid conceptual confusion.

4.2.2 Analysis of the Raw Photodetector Signal

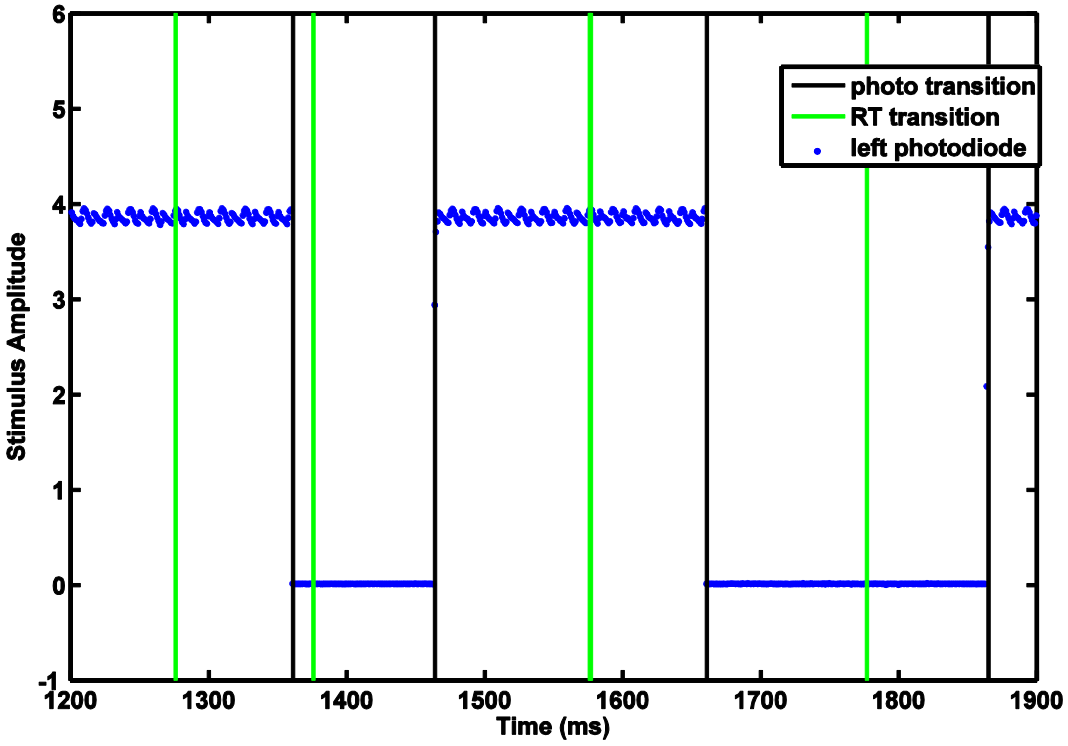

Figure 14. Photodetector signal.

State transitions (horizontal green lines) indicate the time at which the visual display was changed. Following the transition, the raw Photodetector signal (blue) would indicate the change in visual display (horizontal black line).

The behavioral paradigm displayed a white square that alternatively appeared and disappeared to visually indicate a change in state. The phototransistor was positioned over this square and reported when the state change was actually processed and performed. Figure 14 shows the processing of the raw photodetector signal using the function ***PhotoTransitions()***. The function reviews the raw photodetector signal to look for alternations in the high/low status and syncs them to the *stateTransistions* field recorded in the .mat file (table 2). The function only assigns photodetector

times to states within a narrow window of the photo-transition event. In some cases, states are only present for 1ms and do not cause a photo-transition event (for instance state 3 in table 2). In this event, the photo-transition time was assigned to the first state change and the lack of a photodetector signal shift, indicated with a zero, is assigned to the following states.

Table 2. Visual and motor onset times synced with real-time state transition times

State	1	2	3	4	5
RT Time	1276	1376	1576	1577	1777
Photo Time	1361	1464	1661	0	1865
Motor Time	NaN	NaN	NaN	1589	NaN

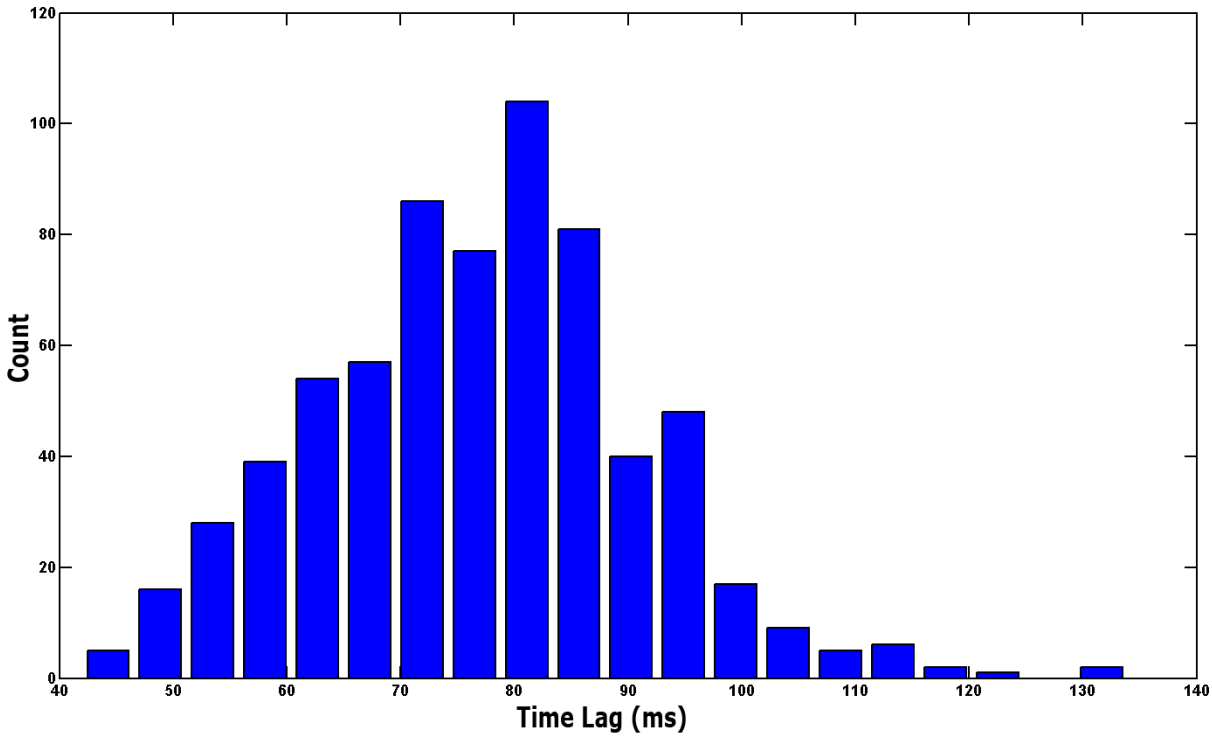

Figure 15. Visual stimulus onset lag.

Due to the graphic processing and screen refresh rate, the disjoint between the command for a visual display and its actual onset can range from 40ms to 100ms with a mean of 77ms (figure 15).

Because of such large lags, any task that utilizes timing of visual stimuli must sync the visual display to the system time; otherwise any behavioral or neurological results linked with the onset of a visual display will be inaccurate by up to 100ms.

4.3 VIBROTACTILE MOTOR ONSET (VIPER BOX)

Tactile stimuli were delivered via a Jameco Reliapro 1.3V 8500RPM vibrating motor. The small pager motor was fixed in a plastic capsule and worn by the subject. During states in which tactile stimulation was administered, a signal from the DAQ card connected host machine sent out a voltage to the VIbrotactile Proprioceptive EmulatoR (VIPER) box, which amplified the signal and powered the motors. Once power was distributed to the motors, they ramped up and provided vibrotactile stimulation of an intensity determined by the input signal. In order to properly sync the tactile stimulation onset with the trail data, this ramp-up time was monitored with accelerometers attached to the motors and relayed the x, y, and z acceleration of the motors to the Host machine.

4.3.1 VIPER Box circuit

The VIPER box consisted of 2 systems: 6 operational amplifiers to control & power 6 motors independently and a power & signal relay system for the 2 accelerometers. Each operational amplifier consisted of the circuit in figure 16. Physically, each integrated circuit contained 2 opamps; only 3 IC were required for the VIPER box. For each IC, an adjustable regulator was used to step down the 24V current from the outlet to 5V for the IC.

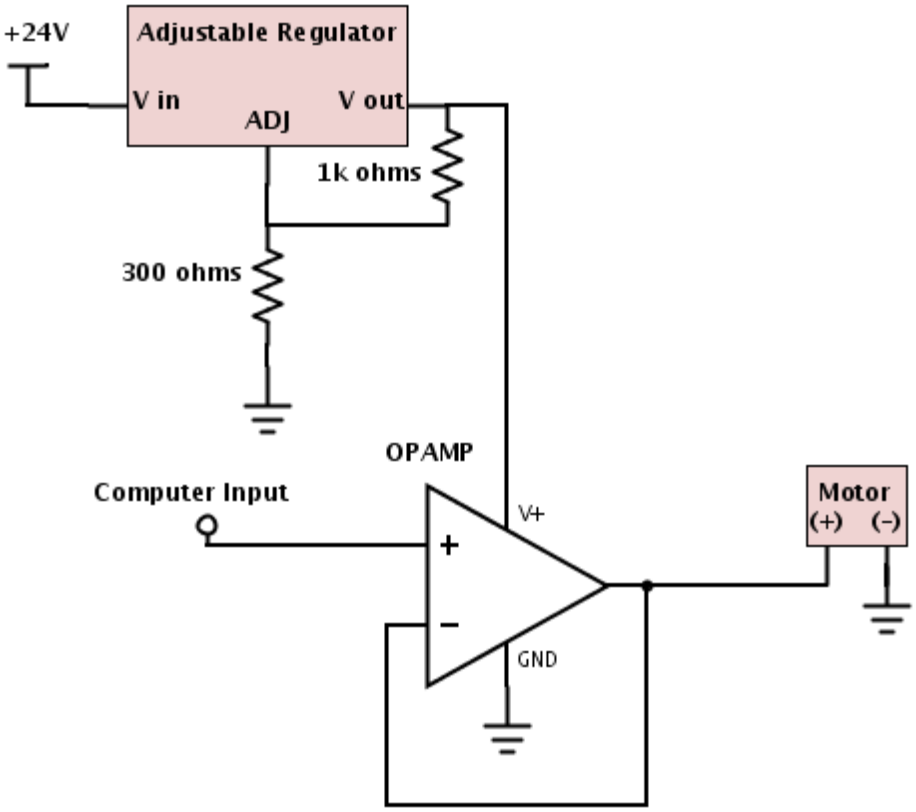

Figure 16. Motor operational amplifier circuit.

Component list:

- Operational Amplifier: TLV4112
- Adjustable Regulator: LM117
- Motor: Jameco Reliapro 1.3V 8500RPM vibrating motor
- Resistors: 1kΩ & 300Ω
- 24V AC/DC Adapter

The accelerometer used was a *triple axis accelerometer breakout board* (MMA7260Q) powered by 5.5V. Output from the x, y, and z accelerometers were relayed independently to the Host machine to be recorded.

4.3.2 Accelerometer Signal Analysis

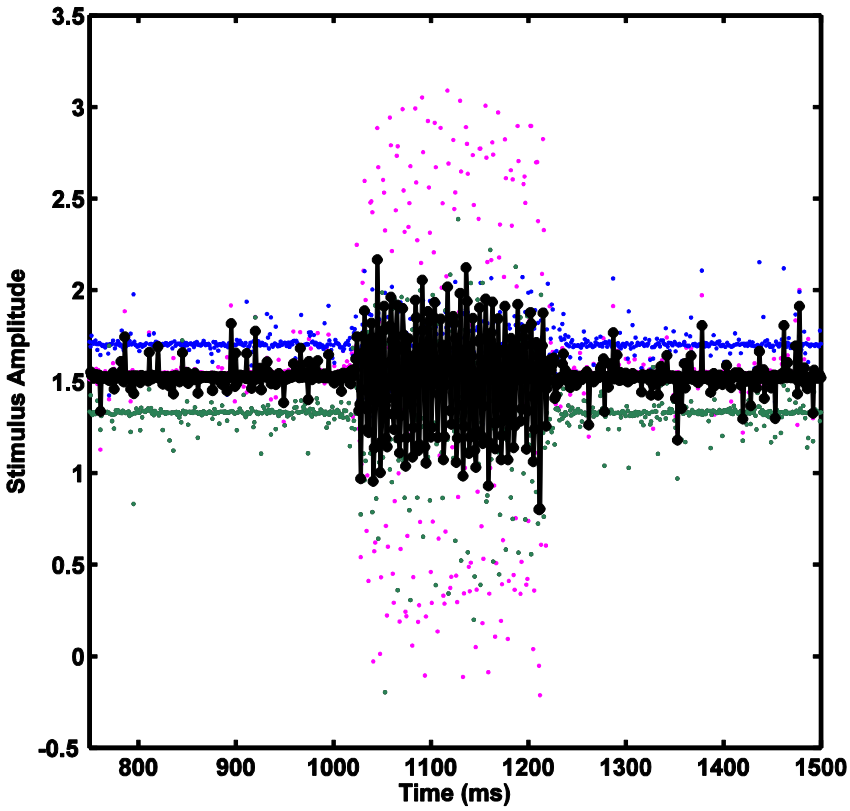

Figure 17. Raw accelerometer signal.

Raw x,y, and z accelerometer signals (blue, green, and purple dots) with signal average (black).

The function ***MotorLatency()*** was used to sync the motor onset times with the Real-Time clock using the accelerometer signals. The accelerometer was placed on the subjects with no regard to the orientation of the x, y, and z direction. While the raw accelerometer values for x, y and z may having distinct values from one another, the orientation could change throughout the day, changing the amplitude and baseline of the signal. In order to sync motor activity, the signals were averaged together to ensure the net disruption from the motor remained consistent throughout the session

(figure 17). The averaged signal was normalized by subtracting the mean signal amplitude across all periods that did not have motor activity. Now that the signal was centered on zero, the absolute value was taken, making periods of motor activity have a much higher value than periods with no motor activity (red points in figure 18). The processed signal was then smoothed to remove the extreme high and low values, and creating a plateau in the signal where the motor activity ramping up could clearly be seen (black points in figure 18). This smoothed signal was very consistent from session to session. When the activity level crossed a threshold of 0.175, it indicated the onset of the motor (Motor time in table 2 and blue star in figure 18).

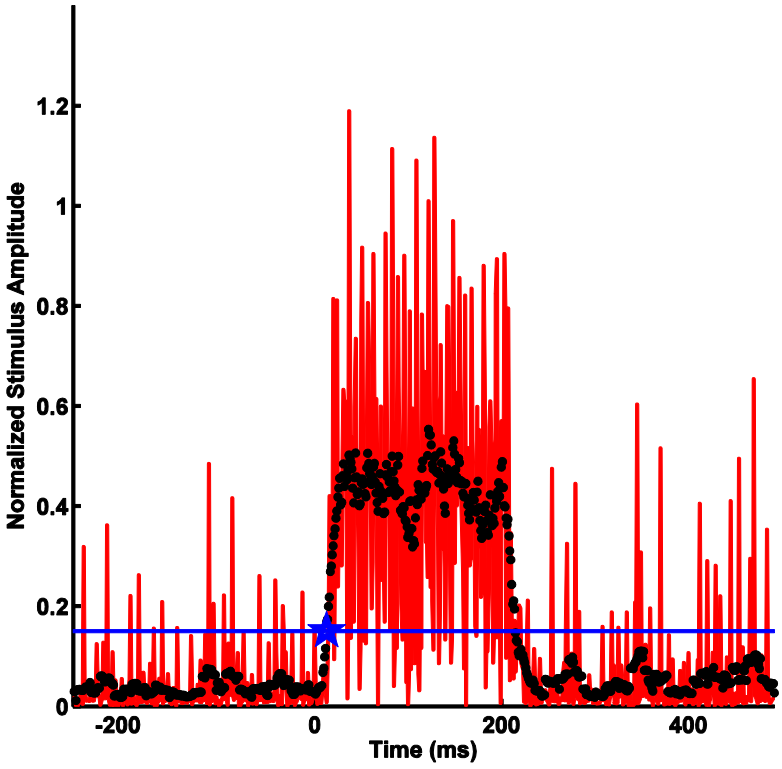

Figure 18. Processed accelerometer signal.

Time 0 indicates the moment the motor was instructed to turn on. Unsmoothed normalized accelerometer signal (red) with smoothed accelerometer signal (black). Threshold level set at .175 (blue line) and a blue star at time when that threshold was crossed, indicating vibrotactile stimulus onset.

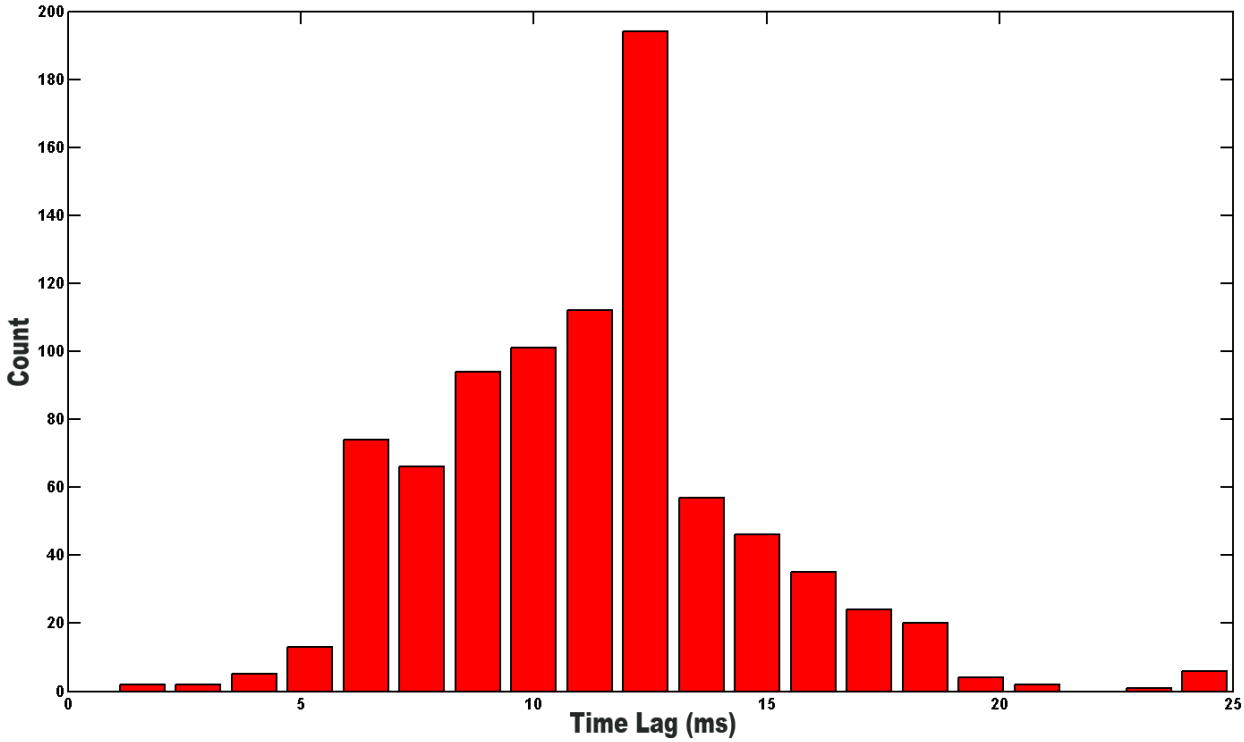

Figure 19. Tactile stimulus onset lag.

The motor ramp up time for the tactile stimuli was very small and relatively consistent compared to the visual stimulus lag. Lags for vibrotactile stimuli ranged from 3ms to 25ms with a mean of 11ms (figure 19). For time critical tasks, the lag is large enough to warrant monitoring; however, the lag is short enough that it can be relied upon to show up within the state that it is called in.

4.4 MICROSTIMULATION AND SINGLE UNIT RECORDING SETUP

The microstimulation and single unit recording system was setup to be easily transportable from rig to rig. With this in mind, the system could be used independently of the Host behavioral

programs and only interfaced with the host computer structure to record and sync data with events during a trial or to trigger microstimulation (figure 20). Listening to and recording single units could even be done with recordings saved onto an SD card and without the Host and Real-Time computers even being on.

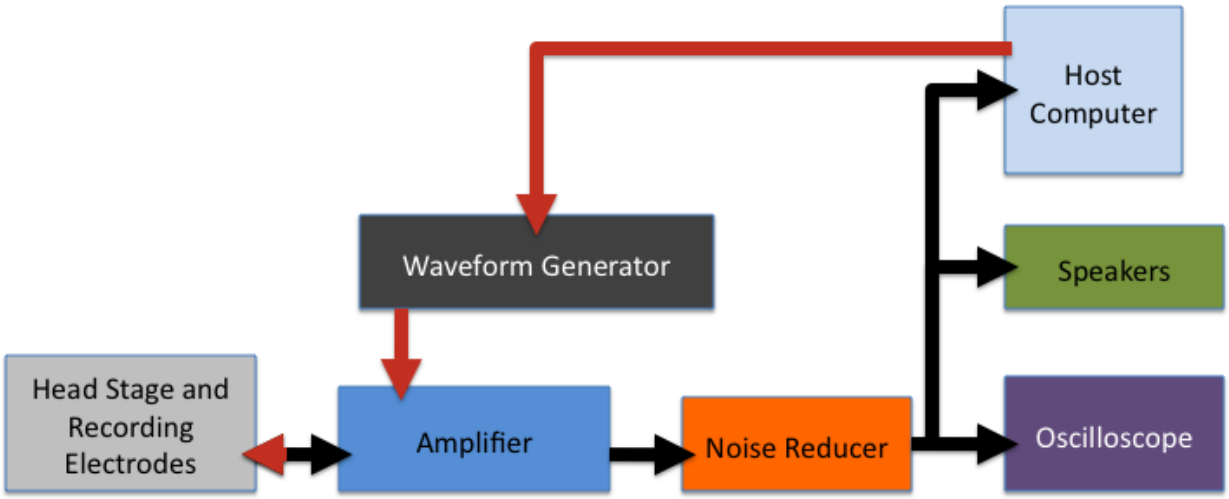

Figure 20. Single unit recording and microstimulation setup.

Microstimulation signal began with a trigger signal, triggering the waveform generator and then progressing to the recording electrodes (red arrows). Recorded activity was sent through a 60Hz noise reducer before being split between an oscilloscope for visualization, speakers and the Host computer to be saved to file (black arrows).

Components:

- Noise Reducer: Humbug 50/60Hz Noise Eliminator
- Microstimulation waveform generator: A-M Systems Model 2100 Isolated Pulse Stimulator, 110V, 60Hz
- Amplifier: A-M Systems 1800 Microelectrode AC Amplifier
- Oscilloscope: Instek GDS-1062A Digital Storage Oscilloscope, 60 MHz

To trigger a microstimulation event, the Host computer sent out a binary TTL pulse to the trigger port of the waveform generator. While the waveform generator is able to generate entire trains of pulses, it can also generate single pulse waveforms allowing for a pseudo Host control over stimulation frequency up to 500Hz. Once the pulse is generated, the signal travels through the amplifier unmodified, then into the head stage and recording electrodes (Figure 20). While the amplifier is in "Stimulus Mode", signals will still be recorded and sent through the output port to monitor microstimulation signals, but neural activity recording quality is drastically reduced. When recording neural activity, the signal travels through the amplifier to a 60Hz noise reducer and then to an oscilloscope for visualization. The signal is also split to speakers for audio monitoring of the signal. This signal can also be sent to the DAQ card on the Host machine in order to record the signals to file. For experiments that do not require recording signals, an easy method for quickly setting up a recording using the Host behavioral software is to plug the speaker output into one of the two Photodetector inputs in the DAQ by either using a spare BNC cable from the Photodetector and plugging it in at the junction of the speaker and the oscilloscope, or simply unplugging the speaker and attaching alligator clips to the audio plug and running the wires to the DAQ. The signal will be recorded on the secondary Photodetector channel (figure 21) and be visualized on-screen. The microstimulation signal itself was analyzed similar to the vibrotactile signal in section 4.3.2 using the matlab function ***MicrostimLatency().*** The lag between triggering a microstimulation event and recording the output of that event on the Host machine was less than 1ms (figure 22). Because of this, during tasks where microstimulation parameters are consistent across the session, the user does not need to record the microstimulation signal in order to properly sync the signal onset with the Real-Time computer time as long as the onset time of the state that triggers the microstimulation is known.

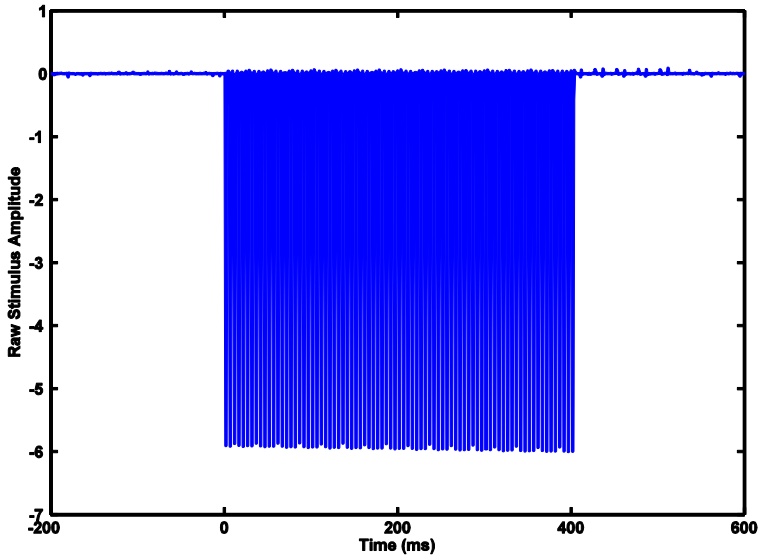

Figure 21. Raw microstimulation signal.

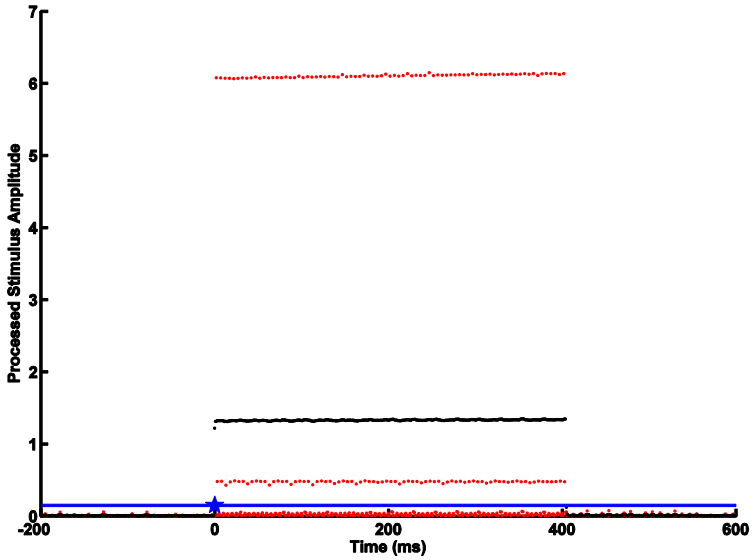

Figure 22. Processed microstimulation signal.

Time 0 indicates the moment the microstimulation was triggered. Unsmoothed normalized microstimulator signal (red) with smoothed microstimulation signal (black). Threshold level set at .175 (blue line) and a blue star at time when that threshold was crossed, indicating microstimulation stimulus onset.

4.5 PHASESPACE-HOST-RT COMMUNICATION LAG

When the Phasespace motion capture system records hand position, it sends those positional coordinates to the host machine, however the Phasespace machine runs on a different internal clock than the Real-Time machine that the behavioral paradigm runs on. In order to sync Phasespace marker data temporally with events happening in the behavioral paradigm a sync signal is introduced. Analyzing these signals compared to how the behavioral paradigm would react in an ideal world reveals some minor system lag that should be kept in mind when analyzing time critical data (figure 23).

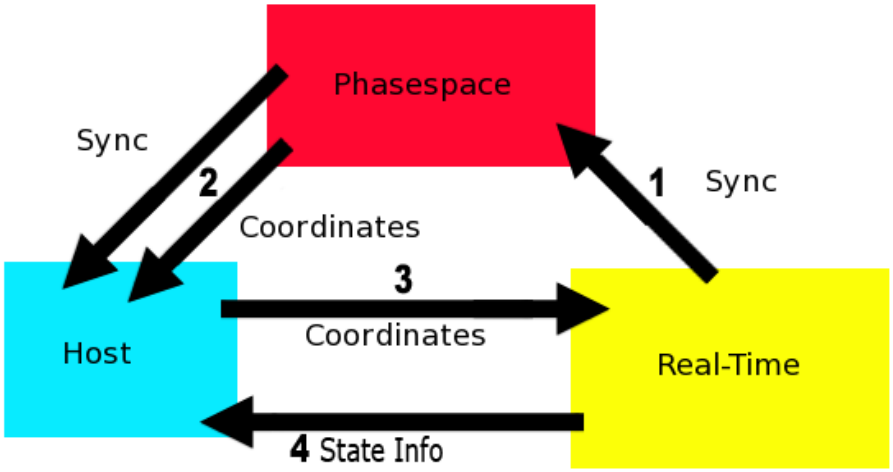

Figure 23. Sync signal and coordinate transmission diagram.

(1) The sync signal is sent from the Real-Time machine to Phasespace and paired with a coordinate sample. **(2)** Phasespace sends the sync signal and coordinate pair to the Host machine to be recorded. **(3)** The Host machine then sends the coordinates to the Real-Time machine to evaluate state conditions and advance the trial. **(4)** Updated State conditions are sent back to the Host machine to be recorded.

While the time between the sync signal being sent from the RT machine to the Phasespace machine is negligible, the time it takes for the coordinates to be sent to the Host machine and then back to the RT machine where the coordinates are analyzed is not. There seems to be a 15ms lag between when a Phasespace marker is reported to have entered a target window to when the RT responds by advancing to the next state. This causes a disjoint between the Phasespace marker times and the *stateTransitions* field in the .mat file structure.

The bottom line is that if you want to know when the hand moves to a specific location in space, say to touch a target, you must look at the raw data values under marker data; do not simply use the state transition time of the state that advances when that target is touched. There is a measurable lag between when a target is touched as reported by Phasespace and when the RT system responds to that touch. This is something to keep in mind when looking at timing properties of reaches in your analysis.

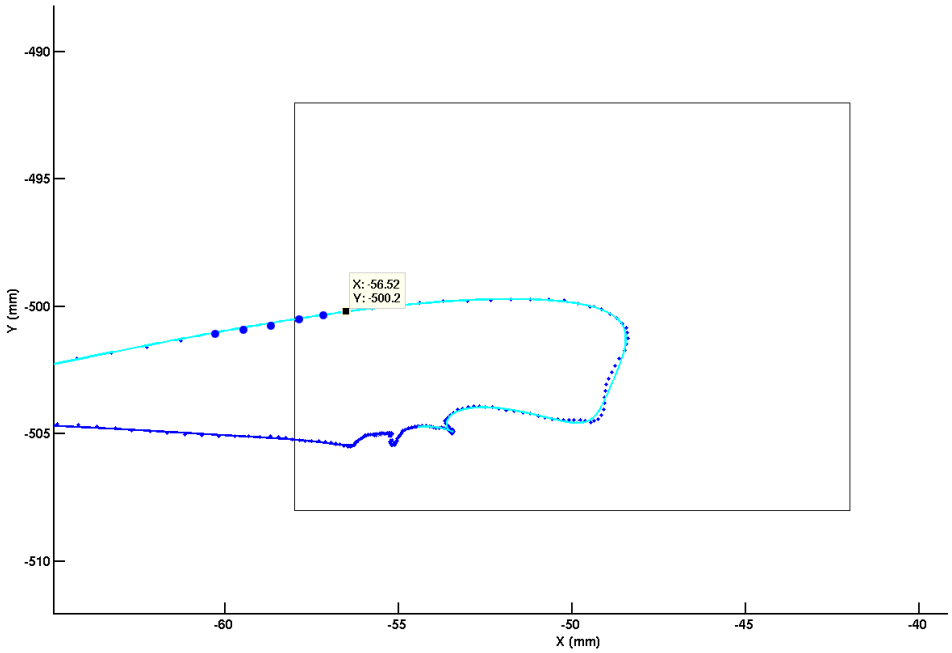

Figure 24. Sample coordinate trace with target crossing.

A sample hand trance with actual Phasespace markers (dark blue dots) synced with the RT time and a smoothed trajectory (light blue line). Reach target is outlined in black. Enlarged blue dots represent samples before and after the hand entered the target. The labeled black square denotes when the RT system recognized the hand entering the target. It should be noted that this occurs 2 samples AFTER the initial sample enters the target boundary.

To illustrate this, figure 24 shows a sample hand trajectory crossing a target threshold The Box shows the target window and the blue dots are raw samples. The first dot that appears inside the box should have triggered a change in state in the rig, however, the time at which a change of state is shown by the labeled black square. Looking at the raw data and keeping in mind that the target boundary is at -58mm (table 3)

Table 3. Raw phasespace marker samples crossing a target threshold

X	Y	Z	Sample Number	Time
-59.52	500.88	151.29	449074	817
-58.73	500.72	151.36	449075	826
-57.96	**500.52**	**151.42**	**449076**	**834**
-57.23	500.32	151.47	449077	842
-56.48	**500.17**	**151.51**	**449078**	**851**
-55.76	500.05	151.54	449079	859

Time the state change should have occurred

Time the Phasespace sync signal says it occurred

The raw data values of the markers show that the target was touched (ie crossing the threshold and having x > 58 and y > 508) at 834, however the file's state transition time for touching the target after being synced with the system time using the sync signal is reported at 851. This lag varies from trial to trial, but is about 10ms 90% of the time as seen in the histogram of figure 25.

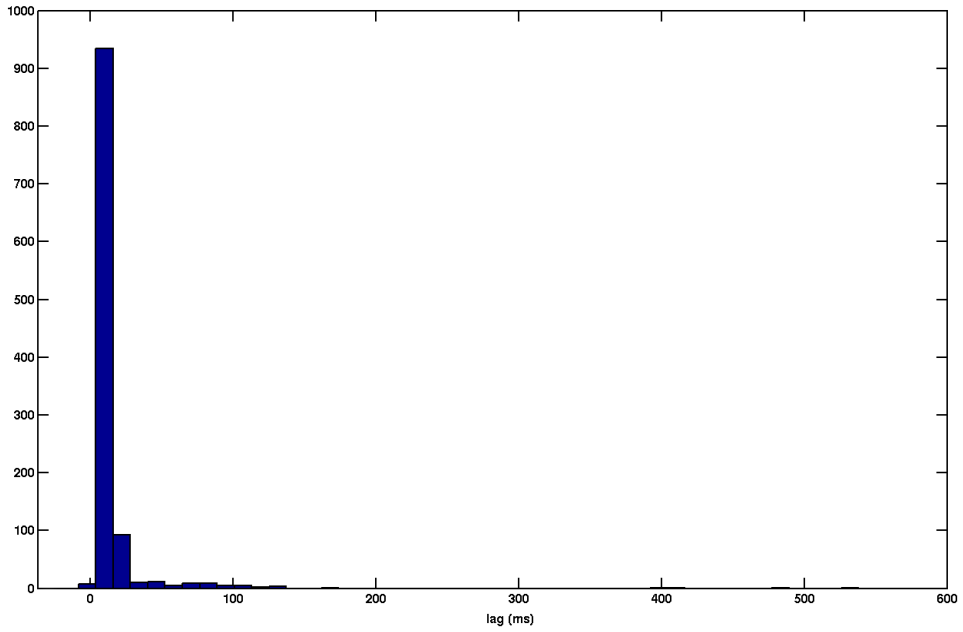

Figure 25. Histogram of time differences between synced marker samples and actual threshold crossings.

What is happening is a Phasespace marker point is being recorded as for example, 100ms into the trial but isn't actually making it to the RT machine to be used for state analysis until 120ms into the trial, thus causing a state transition to be recorded at 120ms even though the data marker being used was captured at 100ms. This makes it difficult to sync the raw Phasespace with the state transitions, which may be important for reaction time studies. However, the transitions of states, while being important for trying to recreate a trial precisely using only the .mat file, are not directly useful for data collection and analysis.

At any given moment, the marker position, neural recording, photodiode reading, and accelerometer are recorded precisely for that specific time point. The only thing that has lag is RT's ability to make decisions based on that data and record that decision at the same time point that the data was received (which is to be expected). This means that while you can't rely on the state transition times to sync up exactly, any state transitions that require precise syncing already have another sync setup already. If something is displayed, it is synced with the photodiode on the screen; if a motor is turned on, the accelerometer reading is recorded, etc. While this isn't detrimental to the data collected or the rig setup, it is something to keep in mind when writing analysis code. State transitions cannot be relied upon to indicate accurate assumptions of Phasespace data.

The functions used to analyze this data were as followed:

FormatPhasespaceData(): to analyze the Phasespace signals based on the sync parameters encoded in the .mat structure.

PhasespaceTransitionSync(): Uses the raw marker samples to manually sync with the threshold crossing of the first target and aligns the rest of the data accordingly.

trialview(): A helpful function that displays all the timing information of a trial as well as hand windows, hand trajectories, raw and smoothed samples, and horizontal & vertical velocities.

5.0 GENERAL DISCUSSION

The central theme behind this dissertation was to access the current capabilities of certain aspects of BCIs and provide a clearer view on how those aspects can be better utilized in the future. We trained two monkeys and ten humans to perform a stimulus response task mid-movement in order to access the effectiveness of visual and tactile stimuli given as feedback cues (Chapter 2). By looking at how rapidly the subjects responded to the cues, we concluded that tactile stimuli could be utilized significantly faster than visual cues. Additionally, the response times between human and monkey were well within the same physiological range. Monkey response times were a little bit faster on average, presumably due to experience with the task. We then took the experiment to the next level by stimulating directly into the brain. We microstimulated in area 1 of the somatosensory cortex, one of the major cortical input areas that signals from tactile stimuli must pass through in order to be perceived. The monkey was able to respond to this microstimulation while in the middle of a reach and could respond fast enough to change an existing motor plan. One unique feature about this task is that the monkey was under pressure to respond to quickly avoid the object that was initially its target. This is promising for using microstimulation as a feedback source. Unfortunately the average response time to microstimulation stimuli was significantly slower and less reliable than to tactile or even visual stimuli. Our results show that, even on a day-to-day basis, microstimulation consistently induced the slowest response times of the three modalities. The utility of microstimulation stimuli also dropped at a much faster rate than the other modalities the closer the reach was to completion. This implies that while microstimulation can be used to convey binary sources of information, it should not be relied upon to deliver quick, clear feedback. Instead, more focus should be placed on using microstimulation

to convey richer data consisting of more than one bit of information in a setting that is not time-critical.

To differentiate the roles and efficacy of multi-unit activity (MUA) and local-field potentials (LFPs) as control signals for brain-computer interfaces, we studied a rich set of MUA and LFP encoding models over non-filtered data. We then determined which of those models best fit the data received from each of these control signals (Chapter 3). We found that while MUA was directionally tuned, as previously reported, it was more strongly tuned to speed. Additionally, this activity was heterogeneous across the electrodes, with some channels providing more speed and directional information than others. Low-frequency LFP activity (LFP_L) was driven predominantly by speed, with activity highly correlated across channels. On the other hand, high-frequency LFP activity (LFP_H) encoded both speed and direction, although directional information was lower compared to MUA. Like MUA, LFP_H activity across electrodes was more heterogeneous than LFP_L. We determined that the most appropriate LFP_L encoding model was a speed only model, whereas a velocity-speed encoding model best described LFP_H tuning. Based on our findings, a hybrid MUA-LFP decoder, accounting for the prominent speed tuning in both neural modalities, should prove superior to velocity-only based decoders.

5.1 DIRECTION OF BRAIN-COMPUTER-INTERFACES

The prospects for brain-computer-interfaces look very exciting in the near future. Cursor control has been obtained with a variety of recording methods like EEG (Onose, et al., 2012), ECoG (Rouse, et al., 2013; Ashmore, et al., 2012), LFP (Flint, et al., 2012), and multi-electrode arrays (Li, et al., 2011; So, et al., 2012). With the needs for rudimentary control satisfied, the technology

has overcome that entry-level barrier of obtaining at least some degree of multi-purpose control and is starting to branch off into different avenues of research like controlling robotic limbs, incorporating different modes of feedback, applications for better communication, aiding in rehabilitation, etc.; much like inventing the first smart phone paved the way for the creation of a wide variety of smart phones available in the market today. It has reached a point where results make the news and begin to create a demand in select patient populations.

Now the emphasis seems to be shifting toward completing the information loop from brain-to-computer-to-brain. Currently this is being attempted by combing previously perfected techniques, like BCI cursor control with microstimulation detection studies. While this doesn't provide a wealth of scientific information beyond proof of concept that two separate working parts also can work together, this is an intriguing and necessary step in the scientific process. First of all, it combines numerous research areas into one neat package, making it easier to draw in public attention, thus allowing more funding to be allocated with the involved areas of research. Second, it is a good tool to reveal unique conflicts involved with combining two technologies from different fields of BCI. One example is microstimulation artifacts interfering with a BCIs decoding ability. While microstimulation is applied, recordings from nearby electrodes for BCI control pick up the microstimulation artifact which distorts recorded activity, lowering quality of control. Because LFP is more consistent across the brain area and less sensitive to individual spikes in activity, it may be a preferable recording method when incorporating these two technologies since the artifact can be more easily removed using filters. This is in contrast to multi-unit recordings where microstimulation stimuli will be incorporated with threshold crossings and also masks naturally occurring spikes at the same time across multiple electrodes and multiple artificially synchronized firing events which need to be removed, thus creating periods of no input during decoding. Lastly,

being in the limelight and having one cutting-edge technology hinge on the reliable success of another cutting-edge technology, exposes the limitations of both technologies and provides inspiration for what needs to be done to improve those technologies independently.

5.2 FUTURE RESEARCH IN MICROSTIMULATION

As microstimulation is increasingly applied as an information channel, the need for a reliable, easily understood stimulus remains (Chapter 2). Currently microstimulation, transcranial magnetic stimulation, and similar modalities are being combined with BCI controlled paradigms to achieve proof of concept confirmation that the two technologies can be combined under one paradigm. As the appeal of being first at combining these two technologies subsides, research will begin focusing on improving the performance of those technologies, particularly in the field of microstimulation, much like the emphasis on different encoding models to achieve greater prediction and control with multielectrode BCIs. Based on my research, this means elucidating the relationship between stimulated area, frequency, pulse waveform, and pattern of somatosensory microstimulation with how quickly and successfully it can be detected.

A key factor in advancing cortical microstimulation will be in eliciting natural looking neural activity so additional cognitive processing does not need to be done in order to utilize the signal. This means that the method of stimulation will need to evolve from an instrument of mass excitation that activates axons, excitatory, and inhibitory neurons indiscriminately. Some degree of selectivity could be achieved through using an asymmetric yet charge balanced waveforms to activate cell bodies but not axons (Wang, et al., 2012). Another option for increased selectivity is

through the adaptation of optogenetics to stimulate the somatosensory cortex. Here specific types of neurons can be tagged and then activated via light through a fiber-optic cable. An additional advantage of this method is the decreased risk of damaging the stimulated tissue. While being able to selectively stimulate a specific population of neurons, currently this method is limited by only being able to activate a small percentage of its target population. This may hinder stimulus perception for use as a fast acting feedback modality, especially so far down stream in the tactile sensory processing chain, where numerous neurons would have been activated from a single tactile stimulus.

Due to the amount of processing already involved once reaching the cortex, it may be advantageous to stimulate peripheral nerves. For users of myoelectric prosthesis, who already have muscle-controlled command over their prosthetic's movement, providing an artificial sense of touch through peripheral nerves would be safer and more appealing than direct cortex stimulation. Smaller amplitude stimulation closer to the cutaneous receptors, the original source of neural signals for tactile stimulation, could provide a more natural sensation than cortical microstimulation for a number of reasons. Being able to both understand and reproduce the patterns of activity is much easier at the receptor level than it is at the cortical level due to the signal being more based on the mechanical aspects of the receptor and less with the neural processing that has already been done. As a tactile stimulus is processed, the number of neurons involved with the signal increases with every synapse; like dropping a stone in a pond, the area disturbed increases with every second that passes. Trying to mimic tactile sensations with cortical microstimulation is like trying to go from calm water to instantaneously emulating the effects of the dropped stone 3 seconds after it was dropped without emulating the previous 3 seconds. It may not be impossible, but the task becomes increasingly difficult the further down the process that

you try to emulate because of the magnitude of factors involved. Stimulating closer to the receptor means it is more probably that one could stimulate the same amount of neurons in a similar fashion as what would have happened with a natural stimulus. Also, it goes without saying, for the chance to have some degree of touch emulated, surgery on the stump of a lost limb is much more appealing than brain implantation.

5.3 FUTURE RESEARCH IN BRAIN-COMPUTER-INTERFACES

Two of the largest confounds with commercializing BCIs today are the high level of invasiveness of the Utah array and the benefits gained from using a BCI. Arguably the best results with control have been obtained with multi-unit activity from multi-electrode arrays implanted in the cortex. Because the array is a foreign object penetrating the brain, the brain mounts a defense, coating the electrodes with glial cells and ejecting it from the tissue. This causes the recording quality of these arrays to degrade over a period of 6 months to 3 years with unpredictable levels of success and an increased level of infection. If an infection does occur, centimeters of brain tissue can be lost causing movement impairment and other problems. In return for taking these risks, BCI users can control a computer cursor, robotic arm, or spell out words on a computer screen. While this control is better than nothing, it is slow, shaky and painful to watch. Communication BCIs move along at 15 words per minute (Santhanam, et al., 2006). In other words, it would have taken 13 minutes to copy this paragraph up to this point. Currently, the risk-benefit ratio is only appealing to those with only the most severe cases of immobility (quadriplegia) and for researchers seeking to further understand brain function or improve BCI decoding ability. With the advent of longer

lasting cortical recording devices for SUA and more specific cortical stimulation techniques, BCI's will be able to offset increased invasiveness with greater performance and capability.

The next steps in BCI research will be to deal with these problems. Each recording modality has a finite limit to the amount of information that can be obtained. As more advance decoding methods are created, they are beginning to hit against a wall of diminishing returns. Chapter 3 clearly shows that different recording modalities contain different types of kinematic information. Future BCIs can capitalize on this by creating combination decoders that utilize multiple modalities of recording signals to improve performance. LFP signals could be used to monitor motor and premotor activity to identify different stages of a movement, (intention to move, initiation of the movement, adjustment of the movement, and completion of the movement), allowing for specific MUA decoding parameters pertaining to the current stage to be keyed up for enhanced decoding ability. ECoG could be placed over areas of the brain where the information gained is near the level of MUA to limit the invasiveness of the BCI implants while optimizing information extraction. Miniaturization of voltage sensitive dye recording could lead to a new recording modality for BCI.

Commercially speaking, the short-term focus of BCI should be to incorporate minimally invasive techniques to a larger population like those with missing limbs through more direct advances in current prosthetics and function restoration. EEG signals are already being incorporated in myoelectric prosthetics; obtaining greater control through nerve cuffs and other limp implants would be a logical step in increasing the marketability of BCIs. For quadriplegics who have more to gain from cortical implants, using a less invasive modality such as ECoG arrays not only would be more appealing for long term use, but also easier to gain government approval. Although one hopes that the coming years will establish more experimentally precise and

commercially reliable tools for recording and manipulating neural circuitry, studies employing BCIs have already contributed much to the livelihood of the subjects involved, and their results will guide future work to further improve the quality of life for those suffering from limited mobility. For most researchers in our field, we dream that one day, future scientists will stand on our shoulders and not only restore lost function but improve upon it.

APPENDIX A

FLASH DRIVE CONTENTS

A Verbatim 8GB flashdrive was appended to this dissertation for the benefit of future Batista lab members who may want to revisit one of the projects that I have taken part it.

Contents:

- 3D Wiimote Calibration
- DIY Playstation Eye Tracker
- Juicer Calibration VI
- LabVIEW Tutorials
- Matlab Functions described in this document along with
    - General Programming Functions
    - General Reach Analysis Functions
    - Redirect and Pressured Reaction Time Functions
- Data Files including:
    - Example data for lag calculation of tactile, visual, and microstimulation
    - Raw Human Data
    - Compressed Monkey Data

BIBLIOGRAPHY

Adams, D. et al., 2011. A watertight acrylic-free titanium recording chamber for electrophysiology in behaving monkeys. *J Neurophysiol,* Volume 106, p. 1581–1590.

Asanuma, H. & Rosén, I., 1972. Topographical organization of cortical efferent zones projecting to distal forelimb muscles in the monkey. *Exp Brain Res.,* 14(3), pp. 243-56.

Asanuma, H. & Sakata, H., 1967. Functional organization of a cortical efferent system examined with focal depth stimulation in cats. *J. Neurophysiol.,* Volume 30, pp. 35-54.

Asher, I., Stark, E., Abeles, M. & Prut, Y., 2007. Comparison of direction and object selectivity of local field potentials and single units in macaque posterior parietal cortex during prehension. *J Neurophysiol,* 97(5), pp. 3684-95.

Ashmore, R. et al., 2012. Stable online control of an electrocorticographic brain-computer interface using a static decoder. *Conf Proc IEEE Eng Med Biol Soc,* Volume 2012, pp. 1740-4.

Bansal, A., Truccolo, W., Vargas-Irwin, C. & Donoghue, J., 2012. Decoding 3d reach and grasp from hybrid signals in motor and premotor cortices: spikes, multiunit activity, and local field potentials. *J Neurophysiol,* 107(5), pp. 1337-55.

Bansal, A., Vargas-Irwin, C., Truccolo, W. & Donoghue, J., 2011. Relationships among low-frequency local field potentials, spiking activity, and three-dimensional reach and grasp kinematics in primary motor and ventral premotor cortices. *J Neurophysiol,* 105(4), pp. 1603-19.

Bartlett, J. & Doty, R., 1980. An exploration of the ability of macaques to detect microstimulation of striate cortex. *Acta Neurobiol Exp (Wars).* , 40(4), pp. 713-27.

Berg, J. et al., 2013 . Behavioral demonstration of a somatosensory neuroprosthesis. *IEEE Trans Neural Syst Rehabil Eng.,* 21(3), pp. 500-7.

Brindley GS & Lewin WS, 1968 . The sensations produced by electrical stimulation of the visual cortex. *J Physiol.,* 196(2), pp. 479-93.

Bruce, C., Goldberg ME, Bushnell, M. & Stanton, G., 1985. Primate frontal eye fields. II. Physiological and anatomical correlates of electrically evoked eye movements.. *J Neurophysiol.,* 54(3), pp. 714-34.

Butovas, S. & Schwarz, C., 2003. Spatiotemporal effects of microstimulation in rat neocortex: a parametric study using multielectrode recordings. *J Neurophysiol.,* 90(5), pp. 3024-39.

Carmena, J. et al., 2003. Learning to control a brain-machine interface for reaching and grasping by primates. *PLoS Biol,* 1(2), p. E42.

Chatterjee, A. et al., 2007. A brain-computer interface with vibrotactile biofeedback for haptic information. *J Neuroeng Rehabil,* p. 4:40.

Clark, K., Armstrong, K. & Moore, T., 2011. Probing neural circuitry and function with electrical microstimulation. *Proc Biol Sci.,* 278(1709), pp. 1121-30.

Cohen, M. & Newsome, W., 2004. What electrical microstimulation has revealed about the neural basis of cognition. *Curr Opin Neurobiol,* 14(2), pp. 169-77.

Cole, J., 1995. *Pride and a Daily Marathon.* s.l.:Bradford Book.

Daly, J., Liu, J., Aghagolzadeh, M. & Oweiss, K., 2012 . Optimal space-time precoding of artificial sensory feedback through mutichannel microstimulation in bi-directional brain-machine interfaces. *J Neural Eng.,* 9(6), p. 065004.

Davis, K. et al., 1998. Phantom sensations generated by thalamic microstimulation. *Nature,* 391(6665), pp. 385-7.

Davis, T., Torab, K., House, P. & Greger, B., 2009. A minimally invasive approach to long-term head fixation in behaving nonhuman primates. *J Neurosci Methods,* 181(1), pp. 106-10.

DeAngelis, G. & Newsome, W., 2004. Perceptual "read-out" of conjoined direction and disparity maps in extrastriate area MT. *PLoS Biol,* 2(3), p. E77.

Diederich, A. & Colonius, H., 2004. Bimodal and trimodal multisensory enhancement: effects of stimulus onset and intensity on reaction time. *Percept Psychophys,* 66(8), pp. 1388-404.

Dinse, H. et al., 1997. Short-term functional plasticity of cortical and thalamic sensory representations and its implication for information processing. *Adv Neurol.,* Volume 73, pp. 159-78.

Dobelle, W. et al., 1976. "Braille" reading by a blind volunteer by visual cortex stimulation. *Nature,* 259(5539), pp. 111-2.

Donoghue, J. & Wise, S., 1982. The motor cortex of the rat: cytoarchitecture and microstimulation mapping. *J Comp Neurol,* 212(1), pp. 76-88.

Doty, R., Larsen, R. & Ruthledge, L., 1956. Conditioned reflexes established to electrical stimulation of cat cerebral cortex. *J Neurophysiol,* 19(5), pp. 401-15.

Doty, R., 1965. CONDITIONED REFLEXES ELICITED BY ELECTRICAL STIMULATION OF THE BRAIN IN MACAQUES. *J Neurophysiol,* Volume 28, pp. 623-40.

Doty, R., 1969. Electrical stimulation of the brain in behavioral context. *Annu Rev Psychol,* Volume 20, pp. 289-320.

Ethier, C., Oby, E., Bauman, M. & Miller, L., 2012. Restoration of grasp following paralysis through brain-controlled stimulation of muscles. *Nature,* 485(7398), pp. 368-71.

Ferrier, D., 1876. *The functions of the brain.* London, UK: Smith, Elder & Co..

Fitzsimmons, N. et al., 2007. Primate reaching cued by multichannel spatiotemporal cortical microstimulation. *J Neurosci,* 27(21), pp. 5593-602.

Flament, D. & Hore, J., 1988. Relations of motor cortex neural discharge to kinematics of passive and active elbow movements in the monkey. *J Neurophysiol,* 60(4), pp. 1268-84.

Flint, R., Wright, Z. & Slutzky, M., 2012. Control of a biomimetic brain machine interface with local field potentials: performance and stability of a static decoder over 200 days. *Conf Proc IEEE Eng Med Biol Soc,* Volume 2012, pp. 6719-2.

Flint, R. et al., 2012. Accurate decoding of reaching movements from field potentials in the absence of spikes. *J Neural Eng,* 9(4), p. 046006.

Forster, B., Cavina-Pratesi, C., Aglioti, S. & Berlucchi, G., 2002. Redundant target effect and intersensory facilitation from visual-tactile interactions in simple reaction time. *Exp Brain Res,* 143(4), pp. 480-7.

Frégnac, Y., Shulz, D., Thorpe, S. & Bienenstock, E., 1988. A cellular analogue of visual cortical plasticity. *Nature,* 333(6171), pp. 367-70.

Fritsch, G. & Hitzig, E., 1870. Uber die elektrische Erregbarkeit des Grosshirns. *Arch. f. Anat,* Volume 37, pp. 300-332.

Fu, Q., Flament, D., Coltz, J. & Ebner, T., 1995. Temporal encoding of movement kinematics in the discharge of primate primary motor and premotor neurons. *J Neurophysiol,* 73(2), pp. 836-54.

Gamlin, P. & Yoon, K., 2000. An area for vergence eye movement in primate frontal cortex. *Nature,* 407(6807), pp. 1003-7.

Georgopoulos, A., Kalaska, J., Caminiti, R. & Massey, J., 1982. On the relations between the direction of two-dimensional arm movements and cell discharge in primate motor cortex. *J Neurosci,* 2(11), pp. 1527-37.

Ghez, C., Gordon, J. & Ghilardi, M., 1995. Impairments of reaching movements in patients without proprioception. II. Effects of visual information on accuracy. *J Neurophysiol,* 73(1), pp. 361-72.

Gilja, V. et al., 2012. A high-performance neural prosthesis enabled by control algorithm design. *Nat Neurosci,* 15(12), pp. 1752-7.

Godde, B., Leonhardt, R., Cords, S. & Dinse, H., 2002. Plasticity of orientation preference maps in the visual cortex of adult cats. *Proc Natl Acad Sci U S A,* 99(9), pp. 6352-7.

Gottlieb, J., Bruce, C. & MacAvoy, M., 1993. Smooth eye movements elicited by microstimulation in the primate frontal eye field. *J Neurophysiol,* 69(3), pp. 786-99.

Graziano MS, Alisharan, S., Hu, X. & Gross, C., 2002 . The clothing effect: tactile neurons in the precentral gyrus do not respond to the touch of the familiar primate chair. *Proc Natl Acad Sci USA,* 99(18), pp. 11930-3.

Graziano, M., Patel, K. & Taylor, C., 2004. Mapping from motor cortex to biceps and triceps altered by elbow angle. *J Neurophysiol,* 92(1), pp. 395-407.

Graziano, M., Taylor, C. & Moore, T., 2002. Complex movements evoked by microstimulation of precentral cortex. *Neuron,* 34(5), pp. 841-51.

Heldman, D., Wang, W., Chan, D. & Moran, D., 2006. Local field potential spectral tuning in motor cortex during reaching. *IEEE Trans Neural Syst Rehabil Eng,* 14(2), pp. 180-3.

Heusler, P., Cebulla, B., Boehmer, G. & Dinse, H., 2000. A repetitive intracortical microstimulation pattern induces long-lasting synaptic depression in brain slices of the rat primary somatosensory cortex. *Exp Brain Res,* 135(3), pp. 300-10.

Histed, M., Ni, A. & Maunsell, J., 2013. Insights into cortical mechanisms of behavior from microstimulation experiments. *Prog Neurobiol,* Volume 103, pp. 115-30.

Hochberg, L. et al., 2012. Reach and grasp by people with tetraplegia using a neurally controlled robotic arm. *Nature,* pp. 485(7398):372-5.

Hochberg, L. et al., 2006. Neuronal ensemble control of prosthetic devices by a human with tetraplegia. *Nature,* 442(7099), pp. 164-71.

Jarosiewicz, B. et al., 2013. Advantages of closed-loop calibration in intracortical brain-computer interfaces for people with tetraplegia. *J Neural Eng,* p. 10(4):046012.

Jazayeri, M., Lindbloom-Brown, Z. & Horwitz GD, 2012. Saccadic eye movements evoked by optogenetic activation of primate V1. *Nat Neurosci.,* 15(10), pp. 1368-70.

Jenkins, W., Merzenich, M. & Recanzone, G., 1990. Neocortical representational dynamics in adult primates: implications for neuropsychology. *Neuropsychologia,* 28(6), pp. 573-84.

Katnani, H. & Gandhi, N., 2012. The relative impact of microstimulation parameters on movement generation. *J Neurophysiol.,* 108(2), pp. 528-38.

Kennedy, P. et al., 2004. Using human extra-cortical local field potentials to control a switch. *J Neural Eng,* 1(2), pp. 72-7.

Kimmel, D. & Moore, T., 2007. Temporal patterning of saccadic eye movement signals. *J Neurosci,* 27(29), pp. 7619-30.

Kim, S. et al., 2008. Neural control of computer cursor velocity by decoding motor cortical spiking activity in humans with tetraplegia. *J Neural Eng,* 5(4), pp. 455-76.

Kiss, Z. et al., 2003. Neural substrates of microstimulation-evoked tingling: a chronaxie study in human somatosensory thalamus. *Eur J Neurosci,* 18(3), pp. 728-32.

Knight, T. & Fuchs, A., 2007. Contribution of the frontal eye field to gaze shifts in the head-unrestrained monkey: effects of microstimulation. *J Neurophysiol.,* 97(1), pp. 618-34.

Koivuniemi, A. & Otto, K., 2011. Asymmetric versus symmetric pulses for cortical microstimulation. *IEEE Trans Neural Syst Rehabil Eng.,* 19(5), pp. 468-76.

Koivuniemi, A. & Otto, K., 2012. *The depth, waveform and pulse rate for electrical microstimulation of the auditory cortex.* s.l., IEEE Eng Med Biol Soc..

Liu, J. & Newsome, W., 2000. Somatosensation: Touching the mind's fingers. *Curr Biol,* 10(16), pp. R598-600.

Liu, J. & Newsome, W., 2006. Local field potential in cortical area mt: stimulus tuning and behavioral correlations. *J Neurosci,* 26(30), pp. 7779-90.

Li, Z., O'Doherty, J., Lebedev, M. & Nicolelis, M., 2011. Adaptive decoding for brain-machine interfaces through Bayesian parameter updates. *Neural Comput,* 23(12), pp. 3162-204.

London, B., Jordan, L., Jackson, C. & Miller, L., 2008. Electrical stimulation of the proprioceptive cortex (area 3a) used to instruct a behaving monkey. *IEEE Trans Neural Syst Rehabil Eng,* 16(1), pp. 32-6.

London, M. et al., 2010. Sensitivity to perturbations in vivo implies high noise and suggests rate coding in cortex. *Nature,* 466(7302), pp. 123-7.

Maunsell JH & Gibson JR, 1992. Visual response latencies in striate cortex of the macaque monkey. *J Neurophysiol.,* 68(4), pp. 1332-44.

Mehring, C. et al., 2003. Inference of hand movements from local field potentials in monkey motor cortex. *Nature Neuroscience,* 6(12), pp. 1253-1254.

Mollazadeh, M. et al., 2011. Spatiotemporal variation of multiple neurophysiological signals in the primary motor cortex during dexterous reach-to-grasp movements. *J Neurosci,* 43(15), pp. 531-43.

Moran, D. & Schwartz, A., 1999. Motor cortical representation of speed and direction during reaching. *J Neurophysiol,* 82(5), pp. 2676-92.

Morasso, P., 1981. Spatial control of arm movements. *Exp Brain Res,* 42(2), pp. 223-7.

Moritz, C., Perlmutter, S. & Fetz, E., 2008. Direct control of paralysed muscles by cortical neurons. *Nature,* 456(7222), pp. 639-42.

Mulliken, G., Musallam, S. & Andersen, R., 2008. Decoding trajectories from posterior parietal cortex ensembles. *J Neurosci,* 28(48), pp. 12913-26.

Murphey, D. & Maunsell, J., 2007. Behavioral detection of electrical microstimulation in different cortical visual areas. *Curr Biol.,* 17(10), pp. 862-7.

Murphey, D. & Maunsell, J., 2008. Electrical microstimulation thresholds for behavioral detection and saccades in monkey frontal eye fields. *Proc Natl Acad Sci U S A.,* 105(20), pp. 7315-20.

Musallam, S. et al., 2004. Cognitive control signals for neural prosthetics. *Science,* 305(5681), pp. 258-62.

Neafsey, E. et al., 1986. The organization of the rat motor cortex: a microstimulation mapping study. *Brain Res,* 396(1), pp. 77-96.

Ni, A. & Maunsell, J., 2010. Microstimulation reveals limits in detecting different signals from a local cortical region. *Curr Biol,* 20(9), pp. 824-8.

Nicolelis, M. et al., 2003. Chronic, multisite, multielectrode recordings in macaque monkeys. *Proc Natl Acad Sci USA,* 100(19), pp. 11041-6.

O'Doherty, J. et al., 2009. A brain-machine interface instructed by direct intracortical microstimulation. *Front Integr Neurosci,* Volume 3, p. 20.

O'Doherty, J. et al., 2011. Active tactile exploration using a brain-machine-brain interface. *Nature,* 479(7372), pp. 228-31.

Ohara, S., Weiss, N. & Lenz, F., 2004. Microstimulation in the region of the human thalamic principal somatic sensory nucleus evokes sensations like those of mechanical stimulation and movement. *J Neurophysiol,* 91(2), pp. 736-45.

Onose, G. et al., 2012. On the feasibility of using motor imagery EEG-based brain-computer interface in chronic tetraplegics for assistive robotic arm control: a clinical test and long-term post-trial follow-up. *Spinal Cord,* 50(8), pp. 599-608.

Paninski, L., 2004. Superlinear population encoding of dynamic hand trajectory in primary motor cortex. *Journal of Neuroscience,* 24(39), pp. 8551-8561.

Paninski, L., Fellows, M., Hatsopoulos, N. & Donoghue, J., 2004. Spatiotemporal tuning of motor cortical neurons for hand position and velocity. *J Neurophysiol,* 91(1), pp. 515-32.

Penfield, W. & Perot, P., 1963. The Brain's Record of Auditory and Visual Experience. A Final Summary and Discussion. *Brain,* Volume 86, pp. 595-696.

Penfield, W., 1958. *The excitable cortex in conscious man.* Liverpool, UK: Liverpool University Press..

Pohlmeyer, E. et al., 2009. Toward the restoration of hand use to a paralyzed monkey: brain-controlled functional electrical stimulation of forearm muscles. *PLoS One,* 4(6), p. e5924.

Prewett, M. S., Elliott, L. R., Walvoord, A. G. & Coovert, M. D., 2012. A Meta-Analysis of Vibrotactile and Visual Information Displays for Improving Task Performance. *IEEE,* 40(1), pp. 123-132.

Prewett, M. S. et al., 2006. The Benefits of Multimodal Information: A Meta-Analysis Comparing Visual and Visual-Tactile Feedback. *ICMI,* pp. 333 - 338.

Rattay, F., 1999. The basic mechanism for the electrical stimulation of the nervous system. *Neuroscience,* Volume 89, pp. 335-346.

Rebesco, J. & Miller, L., 2011. Enhanced detection threshold for in vivo cortical stimulation produced by Hebbian conditioning. *J Neural Eng,* 8(1), p. 016011.

Rickert, J. et al., 2005. Encoding of movement direction in different frequency ranges of motor cortical local field potentials. *J Neurosci,* 25(39), pp. 8815-24.

Robinson, D. & Fuchs, A., 1969. Eye movements evoked by stimulation of frontal eye fields. *J Neurophysiol. ,* 32(5), pp. 637-48.

Robinson, D., 1972. Eye movements evoked by collicular stimulation in the alert monkey. *Vision Res,* 12(11), pp. 1795-808.

Romo, . et al., 2002. From sensation to action. *Behav Brain Res,* 135(1-2), pp. 105-18.

Romo, ., Hernández, A., Zainos, A. & Salinas, E., 1998. Somatosensory discrimination based on cortical microstimulation. *Nature,* 392(6674), pp. 387-90.

Romo, R. et al., 2000. Sensing without touching: psychophysical performance based on cortical microstimulation. *Neuron,* 26(1), pp. 273-8.

Rouse, A., Williams, J., Wheeler, J. & Moran, D., 2013. Cortical adaptation to a chronic micro-electrocorticographic brain computer interface. *J Neurosci.,* 33(4), pp. 1326-30.

Sainburg, R., Ghilardi, M., Poizner, H. & Ghez, C., 1995. Control of limb dynamics in normal subjects and patients without proprioception. *J Neurophysiol,* 73(2), pp. 820-35.

Salzman CD, Britten, K. & Newsome, W., 1990 . Cortical microstimulation influences perceptual judgements of motion direction. *Nature.,* 346(6280), pp. 174-7.

Salzman CD & Newsome WT, 1994. Neural mechanisms for forming a perceptual decision. *Science,* 264(5156), pp. 231-7.

Santhanam, G. et al., 2006. A high-performance brain-computer interface. *Nature,* 442(7099), pp. 195-8.

Schalk, G. et al., 2004. Bci2000: a general-purpose brain-computer interface (bci) system. *IEEE Trans Biomed Eng,* 51(6), pp. 1034-43.

Schiller PH & Sandell, J., 1983. Interactions between visually and electrically elicited saccades before and after superior colliculus and frontal eye field ablations in the rhesus monkey. *Exp Brain Res.,* 49(3), pp. 381-92.

Schiller, P. & Stryker, M., 1972. Single-unit recording and stimulation in superior colliculus of the alert rhesus monkey. *J Neurophysiol.,* 35(6), pp. 915-24.

Scott, J. & Gray, R., 2008. A comparison of tactile, visual, and auditory warnings for rear-end collision prevention in simulated driving. *Hum Factors,* 50(2), pp. 264-75.

Scott, S., Sergio, L. & Kalaska, J., 1997. Reaching movements with similar hand paths but different arm orientations. ii. Activity of individual cells in dorsal premotor cortex and parietal area 5. *Neurophysiol,* 78(5), pp. 2413-26.

Serruya, M. et al., 2002. Instant neural control of a movement signal. *Nature,* Volume 416, p. 141–142.

So, K. et al., 2012. Redundant information encoding in primary motor cortex during natural and prosthetic motor control. *J Comput Neurosci,* 32(3), pp. 555-61.

Sripati AP, et al., 2006. Spatiotemporal receptive fields of peripheral afferents and cortical area 3b and 1 neurons in the primate somatosensory system. *J Neurosci.,* 26(7), pp. 2101-14.

Stark, E. & Abeles, M., 2007. Predicting movement from multiunit activity. *Journal of Neuroscience,* 27(31), pp. 8387-8394.

Stoney, S. J., Thompson, W. & Asanuma, H., 1968. Excitation of pyramidal tract cells by intracortical microstimulation: effective extent of stimulating current. *J Neurophysiol,* 31(5), pp. 659-69.

Strick, P. & Preston, J., 1978. Multiple representation in the primate motor cortex. *Brain Res,* 154(2), pp. 366-70.

Suminski, A. et al., 2011. Continuous decoding of intended movements with a hybrid kinetic and kinematic brain machine interface. *Conf Proc IEEE Eng Med Biol Soc,* pp. 5802-6.

Talwar, S. et al., 2002. Rat navigation guided by remote control. *Nature,* 417(6884), pp. 37-8.

Tanaka, M. & Lisberger, S., 2002. Enhancement of multiple components of pursuit eye movement by microstimulation in the arcuate frontal pursuit area in monkeys. *J Neurophysiol.,* 87(2), pp. 802-18.

Tehovnik, E. & Slocum, W., 2005. Microstimulation of V1 affects the detection of visual targets: manipulation of target contrast. *Exp Brain Res,* 165(3), pp. 305-14.

Tehovnik, E. & Slocum, W., 2007. What delay fields tell us about striate cortex. *J Neurophysiol,* 98(2), pp. 559-76.

Tehovnik, E. et al., 2006. Direct and indirect activation of cortical neurons by electrical microstimulation. *J Neurophysiol,* 96(2), pp. 512-21.

Tehovnik, E., 1996. Electrical stimulation of neural tissue to evoke behavioral responses. *J Neurosci Methods,* 65(1), pp. 1-17.

Treves, A. & Panzeri, S., 1995. The upward bias in measures of information derived from limited data samples. *Neural Computation,* 7(2), pp. 399-407.

VanDerLubbe, R., Jaśkowski, P., Wauschkuhn, B. & Verleger, R., 2001. Influence of time pressure in a simple response task, a choice-by-location task, and the Simon task.. *Journal of Psychophysiology,* pp. 241-255.

Velliste, M. et al., 2008. Cortical control of a prosthetic arm for self-feeding. *Nature,* 453(7198), pp. 1098-101.

Wang, Q., Millard, D., Zheng, H. & Stanley, G., 2012. Voltage-sensitive dye imaging reveals improved topographic activation of cortex in response to manipulation of thalamic microstimulation parameters. *J Neural Eng,* 9(2), p. 026008.

Weber, D., Friesen, R. & Miller, L., 2012. Interfacing the somatosensory system to restore touch and proprioception: essential considerations. *J Mot Behav*, 44(6), pp. 403-18.

Wilson, J., Walton, L., Tyler, M. & Williams, J., 2012. Lingual electrotactile stimulation as an alternative sensory feedback pathway for brain-computer interface applications. *J Neural Eng*, 9(4), p. 045007.

Zhuang, J., Truccolo, W., Vargas-Irwin, C. & Donoghue, J., 2010 . Decoding 3-d reach and grasp kinematics from high-frequency local field potentials in primate primary motor cortex. *IEEE Trans Biomed Eng.*, 57(7), pp. 1774-84.

Zhuang, J., Truccolo, W., Vargas-Irwin, C. & Donoghue, J., 2010. Reconstructing grasping motions from high-frequency local field potentials in primary motor cortex. *Conf Proc IEEE Eng Med Biol Soc*, Volume 2010, pp. 4347-50.